Gobierno de la ciudad de Buenos Aires
Hospital Neuropsiquiátrico "Dr. José Tiburcio Borda"
Laboratorio de Investigaciones Electroneurobiológicas
y Revista

Electroneurobiología

ISSN: 0328-0446

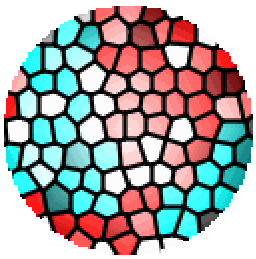

The nervous principle: active versus passive electric processes in neurons

by
Danko Dimchev Georgiev [1]

Correspondencia / Contact: *dankomed [-at--] yahoo.com*

Electroneurobiología 2004; **12** (2), pp. 169-230; URL <http://electroneubio.secyt.gov.ar/index2.htm>

[1] M.D.; Department of Emergency Medicine, Bregalnitsa Street 3, Varna 9000, Bulgaria; Division of Electron Microscopy, Medical University of Varna, Varna 9000, Bulgaria

Abstract: This essay presents in the first section a comprehensive introduction to classical electrodynamics. The reader is acquainted with some basic concepts like right-handed coordinate system, vector calculus, particle and field fluxes, and learns how to calculate electric and magnetic field strengths in different neuronal compartments.

Then the exposition comes to explain the basic difference between a passive and an active neural electric process; a brief historical perspective on the nervous principle is also provided. A thorough description is supplied of the nonlinear mechanism generating action potentials in different compartments, with focus on dendritic electroneurobiology. Concurrently, the electric field intensity and magnetic flux density are estimated for each neuronal compartment.

Observations are then discussed, succinctly as the calculated results and experimental data square. Local neuronal magnetic flux density is less than $^{1}/_{300}$ of the Earth's magnetic field, explaining why any neuronal magnetic signal would be suffocated by the surrounding noise. In contrast the electric field carries biologically important information and thus, as it is well known, acts upon voltage-gated transmembrane ion channels that generate neuronal action potentials. Though the transmembrane difference in electric field intensity climbs to ten million volts per meter, the intensity of the electric field is estimated to be only ten volts per meter inside the neuronal cytoplasm.

Principio del funcionamiento nervioso: oposición de procesos eléctricos activos y pasivos en las neuronas. **Sumario:** Este trabajo presenta en su primera sección una introducción general a la electrodinámica clásica. Cubre los temas electroneurobiológicos introductorios de la mayoría de los cursos de neurociencias, asegurando ante todo la familiaridad del estudiante con los sistemas de coordenadas a mano derecha, así como con el cálculo de vectores y con los flujos de partículas y de campo. En esta sección el lector aprende a calcular las intensidades de campo eléctricas y magnéticas dentro de los diferentes compartimientos neuronales.

Luego la exposición se aboca a explicar la esencial diferencia entre procesos neuroeléctricos pasivos y activos; se provee también una breve perspectiva histórica sobre el principio o fundamento de la función neural. Proporciónase una descripción detallada de los mecanismos no lineares que generan potenciales de acción en los diferentes compartimientos, con énfasis en la electroneurobiología dendrítica. Concurrentemente se estiman la intensidad de campo eléctrico y la densidad de flujo magnético para cada compartimiento neuronal.

Las observaciones son entonces analizadas, sucintamente por cuanto los resultados calculados cuadran bien con los datos experimentales. La densidad local del flujo magnético es menos que $^{1}/_{300}$ de la del campo magnético terrestre, lo que explica por qué cualquier señal magnética útil es sofocada por el ruido ambiental. En contraste, el campo eléctrico porta información biológicamente relevante y, como es muy bien sabido, actúa sobre canales iónicos transmembranales abiertos y cerrados por voltaje, que controlan el potencial de acción de la célula. Aunque la diferencia en la intensidad del campo eléctrico a través de la membrana asciende a diez millones de voltios por metro y aun más, la intensidad del campo eléctrico se estima en sólo diez voltios por metro dentro del citoplasma neuronal.

Нейронный принцип: сравнительное описание активных и пассивных электрических процессов. Резюме: Первая часть представляет собой краткое введение в класическую электродинамику. Здесь приведены общие положения, излагаемые во многих учебниках физики: правоориентированная координатная система, векторное исчисление, поток из частиц и полевый поток. В этой части читатель знакомится со способами вычисления интенсивности электрического и магнитного поля в различных структурах нервной клетки.

Во второй части объясняется различие между активными и пассивными электрическими процессами в нейронах. Эта проблема рассматривается также в историческом аспекте. Представлено подробное описание нелинейных механизмов генерации действующих потенциалов в отдельных структура нервной клетки, и особенно электронейробиологии дендритов. Для каждого органа клетки (дендриты, сома, аксон) вычислены интенсивности электрического и магнитного поля.

Полученные результаты соответствуют экспериментальным данным. Плотность локального магнитого потока нейронов составляет менее $^{1}/_{300}$ плотности магнитного потока Земли. Поэтому шум среды подавляет магнитный сигнал нейрона. Напротив, электрическое поле несет биологически значимую информацию и оказывает влияние на зависящие от разности потенциалов ионные каналы которые генерируют действующие потенциалы нейронов. Несмотря на то, что трансмембранное электрическое поле достигает 10 миллионов В/м, в нейронной протоплазме интенсивность электрического поля составляет лишь 10 В/м.

Table of Contents

1 Classical electrodynamics 173

1.1 Right-handed coordinate systems 173
1.2 Vectors 173
1.3 Gradient 174
1.4 Particle and field fluxes 175
1.5 Electric field 175
1.6 Electric currents 178
1.7 Magnetic field 179
1.8 Electromagnetic induction 181
1.9 Maxwell's equations 182

2 Electric and magnetic fields in neurons 185

2.1 Passive electric properties – cable equation 188
2.1.1 Spread of voltage in space and time 191
2.1.2 Assessment of the electric field intensity 192
2.1.3 Propagation of local electric currents 192
2.2 Active electric properties – the action potential 193
2.2.1 Nernst equation and diffusion potentials 193
2.2.2 Resting membrane potential 194
2.2.3 Generation of the action potential 195
2.3 Dendrites 202
2.3.1 Electric intensity in dendritic cytoplasm 202
2.3.2 Electric currents in dendrites 205
2.3.3 Magnetic flux density in dendritic cytoplasm 205
2.3.4 Active dendritic properties 208
2.4 Neuronal somata 215
2.5 Axons 216
2.5.1 The Hodgkin-Huxley model of axonal firing 217
2.5.2 Passive axonal properties 220
2.5.3 Electric intensity in the axonal cytoplasm 222
2.5.4 Magnetic flux density in axonal cytoplasm 222
2.6 Electric fields in membranes 223

References 224

1 Classical electrodynamics

In order to investigate the electromagnetic field structure in neurons it behooves to be acquainted with the basic mathematical definitions and physical postulates in classical electrodynamics. Before anything else, it is worth pointing out that a quantity is either a *vector* or a *scalar*. Scalars are quantities fully described by a magnitude alone. Vectors are quantities fully described by both a magnitude and a direction. Because we will work mostly with vectors we have to define what is *positive normal* to a given surface s, what is the positive direction of a given contour Γ and what is a right-handed coordinate system.

1.1 Right-handed coordinate systems

Right-handed coordinate system Oxyz is such a system in which if the z-axis points toward your face the counterclockwise rotation of the Ox axis to the Oy axis has the shortest possible path. The positive normal +n of given surface s closed by contour Γ is collinear with the Oz axis of right-handed coordinate system Oxyz whose x- and y-axis lie in the plane of the surface. The positive direction of the contour Γ is the direction in which the rotation of x-axis to the y-axis has the shortest possible path (Zlatev, 1972).

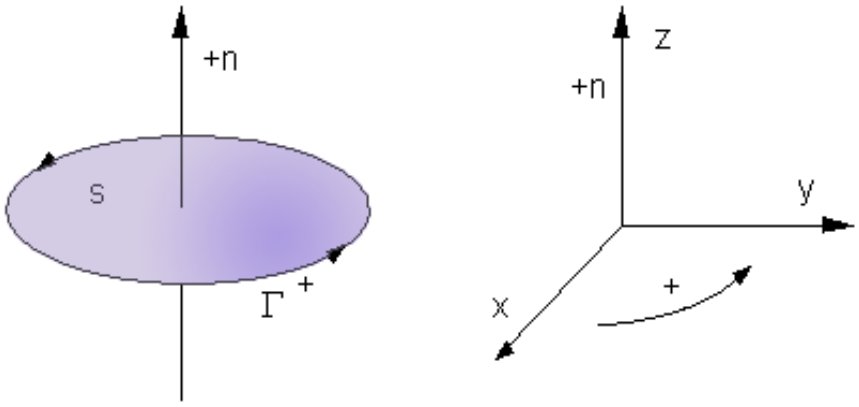

FIG 1 Left: Direction of the positive normal +n and the positive direction of the contour Γ. Right: Right handed coordinate system Oxyz.

1.2 Vectors

After that, for working with vectors it should be noted that there are two types of multiplication of vectors - the dot product and the cross product. Geometrically, the dot product of two vectors is the magnitude of one times the projection of the

other along the first. The symbol used to represent this operation is a small dot at middle height (·), which is where the name *dot product* comes from. Since this product has magnitude only, it is also known as the scalar product:

$$\vec{A} \cdot \vec{B} = A.B.\cos\beta$$

where β is the angle between the two vectors.

Geometrically, the cross product of two vectors is the area of the parallelogram between them. The symbol used to represent this operation is a large diagonal cross (×), which is where the name *cross product* comes from. Since this product has magnitude and direction, it is also known as the vector product:

$$\vec{A} \times \vec{B} = A.B.\sin\beta\vec{n}$$

where the vector $\vec{n}$ is a unit vector perpendicular to the plane formed by the two vectors. The direction of $\vec{n}$ is determined by the right hand rule.

The right hand rule says that if you hold your right hand out flat with your fingers pointing in the direction of the first vector and orient your palm so that you can fold your fingers in the direction of the second vector, then your thumb will point in the direction of the cross product.

1.3 Gradient

The gradient ∇ is a vector operator called *Del* or *Nabla* (Morse & Feshbach, 1953; Arfken, 1985; Kaplan, 1991; Schey, 1997). It is denoted as:

∇ f = grad(f)

The gradient vector is pointing toward the higher values of f, with magnitude equal to the rate of change of values. The direction of ∇ f is the orientation in which the directional derivative has the largest value and $|\nabla f|$ is the value of that directional derivative. The directional derivative $\nabla_u f(x_0,y_0,z_0)$ is the rate at which the function f(x,y,z) changes at a point (x_0,y_0,z_0) in the direction u.

$$\nabla_u f = \nabla f \frac{u}{|u|} = \lim_{h\to 0} \frac{f\left(x + h\vec{u}\right) - f\left(x\right)}{h}$$

and $\vec{u}$ is the unit vector (Weisstein, 2003).

1.4 Particle and field fluxes

The *particle flux* is a scalar physical quantity defined by the expression:

$$\Phi = \lim_{\Delta t \to 0} \frac{\Delta V}{\Delta t},$$

where

$$dV = s\ dl\ \cos\beta$$

dV denotes a *volume segment* with length dl that is filled with *fluid* that for time dt passes with velocity v trough any cross section s of dV ; β is the is the angle between the vectors $\vec{s}$ and $d\vec{l}$. It is worth to remind that $\vec{s}$ has the direction of the positive normal +n, and its magnitude is proportional to the surface area s. Simple substitution of the expression for dV into the expression for Φ gives us

$$\Phi = \vec{v} \cdot \vec{s} = vs\cos\beta$$

Thus we have obtained that the *particle flux* is a scalar product of two vectors - the particle velocity vector $\vec{v}$ and the surface vector $\vec{s}$. In electrodynamics, ion currents in electrolytes and the currents composed of electrons are the particle fluxes of top neurobiological interest, but quasiparticles such as solitons and phonons are also modeled.

We could define an analogous scalar quantity when we investigate physical fields, e.g. the field of electromagnetic force or *electromagnetic field*. There we can define the *field flux* as a scalar product of the field intensity $\vec{A}$ through surface $\vec{s}$.

1.5 Electric field

The electromagnetic force field is composed from the forces of electric and magnetic fields, whose different causal actions can be nonetheless described as mediated by a single sort of microphysical change-causing energy packets, called photons. Taking the photons' action collectively – like as floods can be described by neglecting the swervings of individual water molecules – the electric field could be described via the vector field of electric intensity $\vec{E}$. Electric intensity is defined as the ratio of the electric force $\vec{F}_E$ acting upon a charged body and the charge q of the body:

$$\vec{E} = \lim_{\Delta q \to 0} \frac{\Delta \vec{F}_E}{\Delta q} = \frac{d\vec{F}_E}{dq}$$

It should be noted that the electric field is a potential field – that is, the work W_Γ along closed contour Γ with any length l is zero:

$$W_\Gamma = \oint_\Gamma \vec{F}_E \cdot d\vec{l} = 0$$

Every point in the electric field has an electric potential V defined with the specific (for unit charge) work needed to carry a charge from this point to infinity. The electric potential of point c of a given electric field has potential V defined by:

$$V = \int_c^\infty \vec{E} \cdot d\vec{l} + K$$

where $V_\infty = K = 0$. The electric potential difference between two points 1 and 2 defines voltage V, whose synonyms are electric potential, electromotive force, potential, potential difference, and potential drop:

$$\Delta V = \int_{V_1}^{V_2} dV = \int_1^2 d\vec{E} \cdot d\vec{l}$$

The link between the electric intensity $\vec{E}$ and the gradient of the voltage ∇ V is:

$$\vec{E} = -\nabla V$$

Another vector, not directly measurable, that describes the electric field is the vector of electric induction $\vec{D}$. For isotropic dielectrics electric induction is defined as:

$$\vec{D} = \varepsilon \cdot \vec{E}$$

where ε is the electric permittivity of the dielectric. The electric permittivity of the vacuum is denoted as $\varepsilon_0 = 8.84 \times 10^{-12}$ F/m.

The Maxwell's law for the electric flux Φ_D of the vector of electric induction $\vec{D}$ says that Φ_D through any closed surface s is equal to the located in the space region s charge q that excites the electric field. This could be expressed mathematically:

$$\Phi_D = \oiint_s \vec{D} \cdot d\vec{s} = q$$

If the normal +n of the surface s and the vector $\vec{D}$ form angle β, then the flux Φ_D could be defined as:

$$\Phi_D = \oiint_s \vec{D} \cdot d\vec{s} = \vec{D} \cdot \vec{s} = D.s.\cos\beta$$

$$d\Phi_D = \vec{D} \cdot d\vec{s} = D.ds.\cos\beta$$

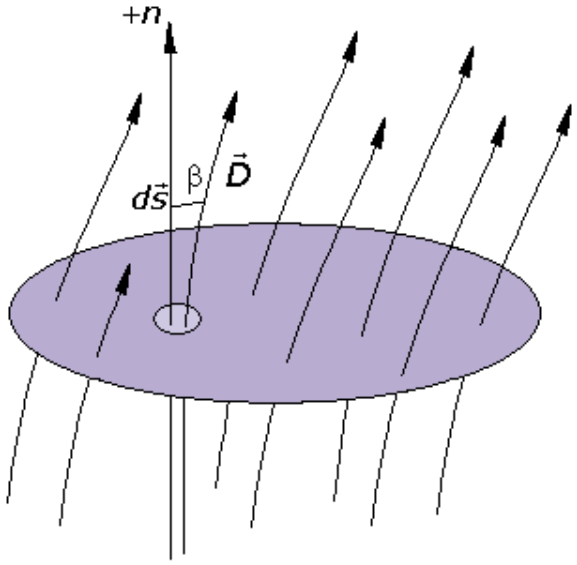

FIG 2 The flux Φ_D of the vector of the electric induction $\vec{D}$ through surface s.

From the Maxwell's law we could easily derive the Gauss' theorem:

$$\Phi_E = \oiint_s \vec{E} \cdot d\vec{s} = \frac{q}{\varepsilon}$$

where Φ_E is the flux of the vector of the electric intensity $\vec{E}$ through the closed surface s.

It is important to note that the full electric flux Φ_D could be concentrated only in a small region Δs of the closed surface s, so in such cases we could approximate:

$$\Phi_D = \iint_{\Delta s} \vec{D} \cdot d\vec{s} = q$$

In other cases, when the electric field is not concentrated in such a small region but we are interested in knowing the partial electric flux $\Delta\Phi_D$ through partial surface Δs for which is responsible electric charge Δq, it is appropriate to use the formula:

$$\Delta\Phi_D = \iint_{\Delta s} \vec{D} \cdot d\vec{s} = \Delta q$$

1.6 Electric currents

The electric current i, that is the flux of physical charges, could be defined by using both scalar and vector quantities (Zlatev, 1972):

$$i = \lim_{\Delta t \to 0} \frac{\Delta q}{\Delta t} = \frac{dq}{dt}$$

$$\vec{i} = \iint_{s} \vec{J} \cdot d\vec{s} = \Phi_J$$

where $\vec{J}$ is the density of the electric current. As a scalar quantity the current density J is defined by the following formula:

$$J = \lim_{\Delta s_n \to 0} \frac{\Delta i}{\Delta s_n} = \frac{di}{ds_n}$$

where s_n is the cross section of the current flux Φ_J. It is useful to note that usually by means of i it is denoted the flow of positive charges. In the description, the flow of negative charges could be easily replaced by a positive current with equal magnitude but opposite direction. Sometimes, however, we would like to underline the nature of the charges in the current. To this purpose we will use vectors with indices, e.g. $\vec{i}_-$ or $\vec{i}_+$, where the direction of the vectors coincides with the direction of motion of the negative or positive charges.

If we have a cable and a current flowing through it, according to Ohm's law the current i is proportional to the voltage V and conductance G and inversely proportional to the resistance R:

$$i = \frac{V}{R} = V.G$$

$$R = \rho \frac{l}{s}$$

$$G = \gamma \frac{s}{l}$$

where ρ is the specific resistance for the media, γ is the specific conductance, l is the length of the cable and s is its cross section.

1.7 Magnetic field

The magnetic field is the second component of the electromagnetic field and is described by the vector of magnetic induction $\vec{B}$ (also known as: magnetic field strength or magnetic flux density) that is perpendicular to the vector of the electric intensity $\vec{E}$. The magnetic field does only act on moving charges. It manifests itself via the magnetic force $\vec{F}_M$ acting upon flowing currents inside the region where the magnetic field is distributed. From Laplace's law it is known that the magnetic force $\vec{F}_M$, which acts upon an electric current-conveying cable immersed in a magnetic field with magnetic induction $\vec{B}$, is equal to the vector product:

$$\vec{F}_M = i \cdot \vec{l} \times \vec{B}$$
$$d\vec{F}_M = i \cdot d\vec{l} \times \vec{B}$$

If we have a magnetic dipole, the direction of the vector of magnetic induction is from the south pole (S) to the north pole (N) inside the dipole – and from N to S outside it.

The magnetic field could be excited either via changes in an existing electric field $\vec{E}$ or by a flowing electric current i. In the first case the magnetic induction is defined by the Ampere's law (in case J = 0):

$$\oint_{\Gamma} \vec{B} \cdot d\vec{l} = \varepsilon_0 \mu_0 \frac{d\Phi_E}{dt}$$

In the second case, if we have a cable with current I, it will generate a magnetic field with magnetic induction $\vec{B}$ whose lines of force have the direction of rotation of a right-handed screw piercing in the direction of the current i.

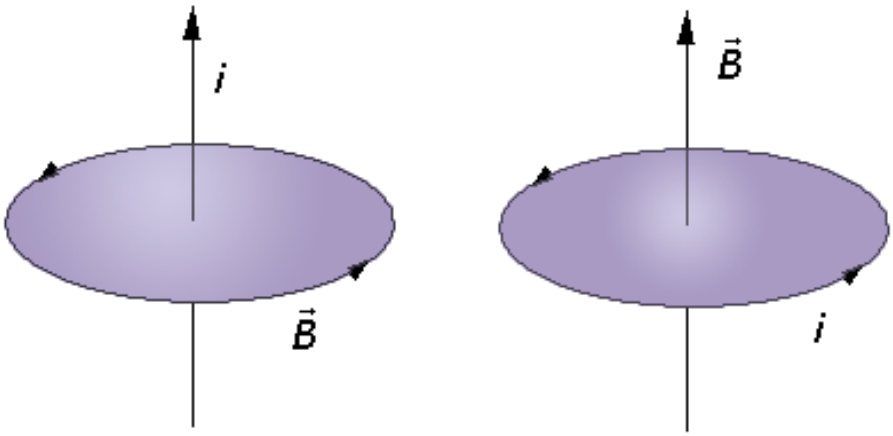

FIG 3 Direction of the lines of magnetic induction around the path axis with current (a) and along the axis of contour with current (b). The current i by convention denotes the flux of positive charges.

The total electromagnetic field manifests itself with a resultant electromagnetic force $\vec{F}_{EM}$ defined by the Coulomb-Lorentz formula:

$$\vec{F}_{EM} = q\left(\vec{E} + \vec{v}_i \times \vec{B}\right)$$

where $\vec{v}_i$ is the velocity of the charge q.

If we have magnetically isotropic media, then we could define another vector describing the magnetic field. It is called magnetic intensity $\vec{H}$, tantamount to

$$\vec{H} = \frac{\vec{B}}{\mu}$$

where μ is the magnetic permeability of the media. The magnetic permeability of the vacuum is denoted with $\mu_0 = 4\pi \times 10^{-7}$ H/m.

The circulation of the vector of magnetic intensity along the closed contour Γ_1 with length l, which interweaves in its core the contour Γ_2 with current i flowing through Γ_2, is defined by the formula:

$$\oint_{\Gamma_1} \vec{H} \cdot d\vec{l} = i$$

It can be seen that the magnetic field is a non-potential field, since the lines of field intensity $\vec{H}$ are closed and do always interweave the contour with the excitatory current i. The circulation of the vector $\vec{H}$ will be zero only along the closed contours which do not interweave in their cores any current i (Zlatev, 1972).

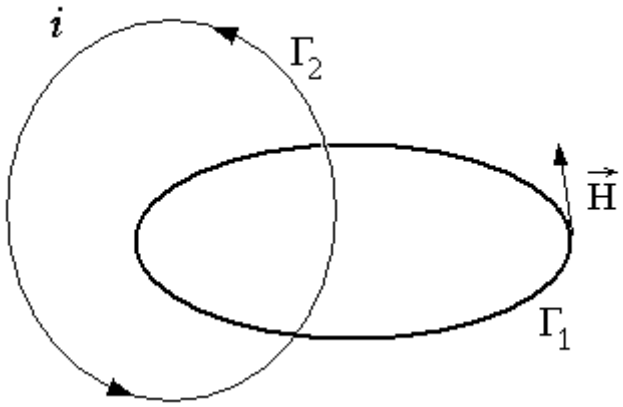

FIG 4 The circulation of the vector of magnetic intensity $\vec{H}$ along the closed contour Γ_1 equals the current i flowing through the interweaved contour Γ_2.

1.8 Electromagnetic induction

Analogously to defining the flux Φ_D of the vector of the electric induction $\vec{D}$ we can define the flux Φ_B of the vector of the magnetic induction $\vec{B}$:

$$\Phi_B = \iint_S \vec{B} \cdot d\vec{s}$$

It is useful to know that the change in magnetic flux generates induced voltage V according to the Lenz's law:

$$V = -\frac{d\Phi_B}{dt}$$

$$\oint_{\Gamma} \vec{E} \cdot d\vec{l} = -\frac{d\Phi_B}{dt}$$

Thus the Lenz's law shows that there will be induced voltage (and therefore electric current) if there is a static cable inside changing magnetic field:

$$V = -\iint_s \frac{\partial \vec{B}}{\partial t} \cdot d\vec{s}$$

or if the cable is moving inside a static magnetic field:

$$V = -\left(\vec{v} \times \vec{B}\right)\vec{l}$$

The full magnetic flux Φ_L of the magnetic field self-induced by a contour with current i is called self-induced flux. The self-induced flux is a linear function of the current:

$$\Phi_L = L \cdot i$$

where L is scalar known as self-inductance and depends only on the magnetic permittivity μ of the media and the geometric parameters Π_L that determine the size and the shape of the contour:

$L = f(\mu, \Pi_L)$

Self-induced voltage appears on electric wires every time that there is a change of the current i – and this self-induced voltage opposes to the change of the current:

$$V = -L\frac{di}{dt}$$

1.9 Maxwell's equations

We have up till now presented the basic principles of electromagnetism. In order to summarize them it is useful to write down the Maxwell's equations. Although these equations have been worked out more than a century ago they present in concise form the whole electrodynamics. We will consider two cases: (i) in the absence of magnetic or polarizable media and (ii) with magnetic and/or polarizable media.

In absence of magnetic or polarizable media the equations can be written in both forms, i.e. in integral or differential form. They will be listed on the following table.

Table 1 Maxwell's equations in the absence of magnetic or polarizable media.

Laws	Integral form	Differential form
Gauss' law for electricity	$\oiint_s \vec{E} \cdot d\vec{s} = \frac{q}{\varepsilon_0}$	$\nabla \cdot E = \frac{\rho}{\varepsilon_0} = 4\pi k \rho$ where ρ is the charge density and $k = \frac{1}{4\pi\varepsilon_0}$ is the Coulomb's constant.
Gauss' law for magnetism	$\oiint_s \vec{B} \cdot d\vec{s} = 0$	$\nabla \cdot B = 0$
Faraday's law of induction	$\oint_\Gamma \vec{E} \cdot d\vec{l} = -\frac{d\Phi_B}{dt}$	$\nabla \times E = -\frac{\partial B}{\partial t}$
Ampere's law	$\oint_\Gamma \vec{B} \cdot d\vec{l} = \mu_0 i + \frac{1}{c^2}\frac{\partial}{\partial t}\oint_\Gamma \vec{E} \cdot d\vec{l}$	$\nabla \times B = \frac{J}{\varepsilon_0 c^2} + \frac{1}{c^2}\frac{\partial E}{\partial t}$

In the cases where a magnetic and/or polarizable medium steps in, the above equations must be re-written in order to take into account the processes occurring inside the medium. We will write down the differential form of the laws.

The Gauss' law for electricity takes the form:

$$\nabla \cdot D = \rho$$
$$D = \varepsilon_0 E + P$$

where P denotes the polarization. For free space we have D = ε_0E and for isotropic linear dielectric D = ε·E. If a material contains polar molecules, when no electric field is applied they will generally be in random orientations. An applied electric field will polarize the material, by orienting the dipole moments of polar molecules. This decreases the effective electric field between the plates and increases the capacitance of the parallel plate structure.

The Gauss' law for magnetism remains in the same form:

$$\nabla \cdot B = 0$$

as well as the Faraday's law of induction:

$$\nabla \times E = -\frac{\partial B}{\partial t}$$

The Ampere's law could rather be written in the form:

$$\nabla \times H = J + \frac{\partial D}{\partial t}$$
$$B = \mu_0 \left(H + M \right)$$

where M denotes the magnetization. For free space we have B = μ_0H and for isotropic linear magnetic medium B = μH. In matter the orbital motion of electrons creates tiny atomic current loops, which produce magnetic fields. When an external magnetic field is applied to a material, these current loops will tend to align in such a way as to oppose the applied field. This may be viewed as an atomic version of Lenz's law: induced magnetic fields tend to oppose the change, which created them. The materials whose only magnetic response is this effect are called diamagnetic. Therefore all materials are inherently diamagnetic, but if the atoms have some net magnetic moment as in paramagnetic materials, or if there is long-range ordering of atomic magnetic moments as in ferromagnetic materials, these stronger effects are always dominant (Nave, 2003).

It is of interest to note that the three basic physical constants in electromagnetism, namely electric permittivity of vacuum, magnetic permeability of vacuum and velocity of light in vacuum, are linked by the equation:

$$\varepsilon_0 \mu_0 c_0^2 = 1$$

This equation exposes a crucial fact, which shows that in electrodynamics the minimal number of physical units is four: length, time, mass and charge.

Taking into account the presented basic laws of classical electrodynamics, we could now try to model the electromagnetic field structure and effects taking place in the different compartments of neural cells - dendrites, soma and axons.

2 Electric and magnetic fields in neurons

The earliest ideas about the nature of the signals in the nervous system, going back to the Greeks, involved notions that the brain secretes fluids or "spirits" that flow through the nerves into the muscles. A new era, nevertheless, opened in 1791 when Luigi Galvani of Bologna showed that frog muscles could be stimulated by electricity (Galvani, 1791). His postulate of the existence of "animal electricity" in nerves and muscles soon led to a focus of attention almost exclusively on the electrical mechanisms for nerve signaling.

In 1838 Carlo Matteucci detected currents in the nerves of the electric fish and pointed out "the greatest analogy that we have between the unknown force in nerves and that of electricity" (Matteucci, 1838). In the 1840s Matteucci observed that when an amputated frog's leg was placed in contact with another leg undergoing contractions, it would contract as well. Using this organic "device", Matteucci discovered an ongoing current in frog muscle, which he could detect with particular clarity in cases of injury (Matteucci, 1840, 1844).

In spite of these first experimental results, the nature of the neural signals remained disputable. In early 1841, the Berlin physiologist and anatomist Johannes Müller presented his twenty-three-year-old medical student Emil Du Bois-Reymond with Matteuci's results and asked Du Bois-Reymond to establish, once and for all, whether the nervous principle was electrical in nature. Müller himself had his doubts. Several facts suggested a fundamental difference between neural and electrical signals: (i) a ligated (tied or crushed) nerve could conduct electricity but could not transmit the nervous principle, (ii) many other types of stimuli besides electricity could excite nerves, giving rise to the nervous principle, and (iii) other moist animal tissues, too, could conduct electricity as suitably as the nervous tissue, if not better. Du Bois-Reymond was to repeat, verify, and extend Matteuci's experiments on the electrical properties of frog muscles. After seven years of hard work he prepared a comprehensive description (in fact a text of about 800 pages) explaining in minute detail the performed experiments. As an appendix, it offered an extensive series of plates illustrating the most important experimental setups, instruments, and frog preparations (Du Bois-Reymond, 1848). In 1850s, Reymond's slightly younger colleague Hermann von Helmholtz, later a famous physicist, was able to measure the speed of conduction of the nerve impulse. He showed for the first time that, though fast, it is not all that fast. In the large nerves of the frog it moves at about 40 meters per second, which is about 140 kilometers per hour (von Helmholtz, 1850; 1852;

1854). This was another landmark finding, as it showed that the mechanism of the nerve impulse has to involve something more than merely the physical passage of electricity as through a wire; it has to involve an *active biological process*. Therefore the impulse eventually came to be called *action potential*.

The ability of a nerve to respond to an electrical shock with an impulse is a property referred to as *excitation*. It thus has been frequent to say that the nerve is *excitable*. Yet in the earliest experiments there were no instruments for recording the impulse directly; it could be detected only by means of the fact that, if a nerve was connected to its muscle, after a brief period for conduction in the nerve the shock was followed by a twitch of the muscle. The fleeting nature of the twitch indicated that an impulse must also occur in the muscle, so that the muscle was also recognized as having the said property of *excitability*. The electrical nature of the nerve impulse and its *finite speed of conduction* were important discoveries for physiology in general – indeed, for articulating several fields of scientific endeavor – because they constituted the first direct evidence for the kind of activity present in the nervous system.

In addition, the fact that the impulse moves at only moderate speed had tremendous implications for psychology, for it seemed to break the mind away from the actions that the mind wills. In effect, it provided empirical evidence understood as supporting the idea of dualism – namely, that the mind is separate from the body. It was one of the stepping-stones toward the development of modern psychology and study of behavior, as well as added fuel for the debate about the nature and relationships of mind and body (Shepherd, 1994).

Between September 1883 and May 1884 Alberto Alberti kept alive and almost daily mapped an exposed human brain as regards sensations and movements stirred through electricity (Alberti, 1884; 1886; Crocco & Contreras, 1986a; Crocco, 1994; Petrolli, 2001) and since then and until 1912 Richard Sudnik, the researcher that had found the proper values of current used by Alberti (Crocco & Contreras, 1986b), published some fifty research papers on electrotherapeutics including probings in the electrical nature of the nervous principle. His friend d'Arsonval (1896) observed phosphenes, dizziness and some people fainting away as their head got into an induction coil and in 1902, in Wien, Bertold Beer and his collaborator Adrian Pollacsek patented an improved therapeutic device (*cf*. Beer 1902) using this effect – while, in turn, various researchers had been probing the motor side, as summarized by Lucien Lamacq (1897). Since 1906 Christfried

Jakob (Jakob, 1906-1908; Barlaro, 1909) started his interference models, of correlogram and hologram-like structure, for depicting – on the many scales of the brain histoarchitectures and anatomical organizations (reverberating "macrocircuits" and "microcircuits") he was uncovering – the formation and spread of global patterns ("stationary waves") of nervous activity, reputed electrical. Ascertaining directly its exact nature took, still, some time.

In 1939 K.C. Cole and H.J. Curtis at Woods Hole introduced in neurophysiological research the use of squids as experimental animals. On the mollusks' very wide axons, the researchers became able to show that membrane resistance decreases during passage of action potential (Cole & Curtis, 1939). They showed that not only does the membrane depolarize (in other words, become less negative inside), but it passes zero and actually becomes almost 50 mV positive inside, at the *peak of the action potential* (Curtis & Cole, 1940; 1942).

A conclusive proof that the action potential is *a membrane event* and it consists of a transient change in the membrane potential came in 1961 by P.F. Baker, A.L. Hodgkin and T.I. Shaw. As we saw this was already assumed or suspected in the nineteenth century; it finally became directly, and elegantly, demonstrated on squid axons, where impulses continue to be conducted even though all the axoplasm has been squeezed out (Baker, P.F. et al. 1961; 1962a; 1962b; 1964).

In order to better explain in the next sections the difference between passive and active electric processes that take part in neurons it is useful to define the terms *passive* and *active*.

Passive electric neuronal process – a process that dissipates the applied potential V_0 as it propagates in space and time. The spread of the electromagnetic field occurs with very high velocity v, which in low loss, non-magnetic materials according to Gary R. Olhoeft (2003) can be nicely approximated by:

$$v \approx \frac{c}{\sqrt{\varepsilon_r}},$$

where c is the *speed of light in vacuum* and ε_r is the *relative dielectric permittivity* (relative to that in free space).

Active electric neuronal process – a process that is fueled with energy (in vivo the ultimate source is ATP) so that either the applied potential V is augmented or it is

transmitted along the projection without decrement. Without an energy source the active process cannot be performed, since it must violate the second law of thermodynamics.

If we investigate only the *passive properties* of a segment of neuronal projection it can be shown that the applied voltage V_0 at certain point x_0 spreads along the projection (approximately with the speed of light in vacuum divided by the square root of the relative dielectric permittivity ε_r) and it decrements exponentially in space. What is important, however, is that the *peak amplitude* of the voltage V does not propagate in space and remains at x_0 (but decrementing in time!).

In contrast, if we consider an *excitable* (that is, active) *segment* of a neuronal projection with voltage sensitive ion channels in the membrane of the projection, and we apply voltage V above certain threshold, then the membrane resistance R_m changes in time as a function of V. In other words, a non-linear process is started. The applied voltage V could be augmented until it reaches a maximal value V_{max} Then this peak amplitude could propagate along the projection as a *solitary wave*.

2.1 Passive electric properties – cable equation

If we investigate only passive electric properties of neuronal projections we could model each neurite as an *electric cable*. Usually the neuronal membrane could be replaced with its equivalent electric schema, which takes into account only the passive properties of the membrane. The simulations of dendrites or axons that take into account only the passive membrane properties show that the electric potentials decrement as they propagate along the neuronal projection. The potential drop (voltage) along the projection induces electric currents that (i) flow along the projection and (ii) leak out through the membrane. Such passive spread of the electric potential is called *electrotonic conductivity* and the equation describing the decrement of the applied potentials in space and time is known in the literature as the *cable equation*. The *peak amplitude* of the applied voltage V, however, remains that at the point of application, x_0.

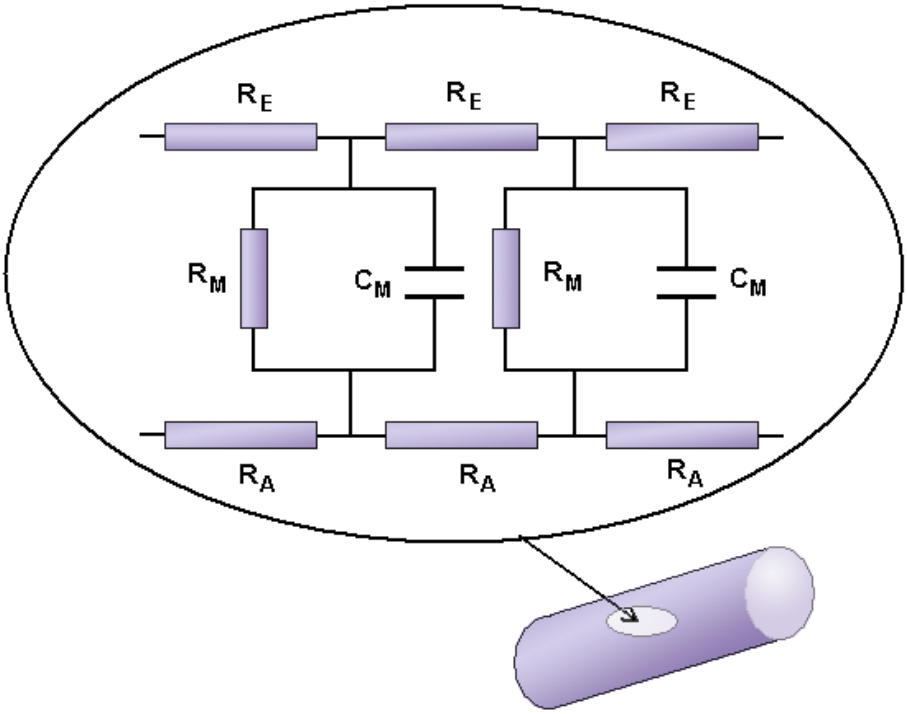

FIG 5 Equivalent electric schema of passive neuronal membrane.

It should be noted that the passive electric properties of the neuronal projections are different for axons, dendrites and neuronal somata. They depend not only on *specific physical constants* (usually defined for unit length or unit volume) of the organic substances that build up the investigated neuronal element, but also depend on *geometric parameters*. On the next table the main parameters of a passive neuronal projection are presented, as well as their symbols and SI units for measurement; brief characterizations are also given.

Table 2 Units of the passive membrane.

Symbol	SI units	Physical meaning	Notes
R_a	Ω	Axial (intracellular) resistance	For a segment of cable with a *fixed* length and *fixed* diameter
R_e	Ω	Extracellular resistance	
R_m	Ω	Membrane resistance	
C_m	F	Membrane capacitance	
r_i	Ω/m	Cytoplasmic resistivity	For unit length of cable with *fixed* diameter
r_e	Ω/m	Extracellular resistivity	
r_m	Ω.m	Membrane resistivity	
c_m	F/m	Membrane capacitance	
R_A	Ω.m	Specific axial resistance	For unit length and unit diameter (i.e. unit volume or surface area of cable)
R_E	Ω.m	Specific extracellular resistance	
R_M	$\Omega.m^2$	Specific membrane resistance	
G_M	S/m^2	Specific membrane conductance	
C_M	F/m^2	Specific membrane capacitance	
V_m	V	Transmembrane voltage	

These physical parameters are linked according to the following equations:

$$R_a = r_i l = \frac{4l}{\pi d^2} R_A$$

$$R_m = \frac{r_m}{l} = \frac{R_M}{\pi d l}$$

$$C_m = c_m l = \pi d l C_M$$

where d is the *diameter* of the neural projection and l is its *length*.

Some of the *specific parameters* were experimentally estimated for real neurons. The *specific axial resistance* R_A is 0.6-1 Ω.m (Miller, 1980; Miller et al., 1985; Fleshman et al., 1988). The value of the *specific membrane resistance* R_M is 0.5-10 Ω.m^2 (Miller et al., 1985; Cauller, 2003) and for the *specific membrane capacitance* C_M it is 0.01 F/m^2 (Miller et al., 1985).

If we introduce a rectangular electric impulse with voltage V, then the voltage across the membrane changes according to the cable equation:

$$-\lambda^2 \frac{\partial^2 V}{\partial x^2} + \tau \frac{\partial V}{\partial t} + V = 0$$

where

$$\tau = r_m c_m = R_m C_m = R_M C_M$$

is the *time constant* (τ) and

$$\lambda^2 = \frac{r_m}{r_i + r_e}$$

is the square of the *space constant* (λ). In neurons $r_i >> r_e$ (Sajda, 2002) so we can write:

$$\lambda = \sqrt{\frac{r_m}{r_i}} = \sqrt{\frac{dR_M}{4R_A}}$$

The cable equation describes the distribution of the membrane potential in space and time if a hyperpolarizing or a depolarizing impulse is applied (Stoilov et al., 1985).

The time constant (τ) and the space constant (λ) have the meaning respectively of time and distance for which the electric voltage V changes e = 2,72 times.

2.1.1 Spread of voltage in space and time

In a given point of time the distribution of the voltage along the dendrite is obtained by the cable equation with V≠f(t) and ∂V/∂t=0:

$$\lambda^2 \frac{\partial^2 V}{\partial x^2} + V = 0$$

The solution of this differential equation is:

$$V_{(x)} = V_0 \exp\left(-\frac{x}{\lambda}\right) + V_1 \exp\left(+\frac{x}{\lambda}\right)$$

The second part of the equation $V_1 \exp\left(+\frac{x}{\lambda}\right)$ could be missed (Stoilov et al., 1985) because it leads to unphysical results when x → ∞. Thus we could just write:

$$V_{(x)} = V_0 \exp\left(-\frac{x}{\lambda}\right)$$

where for V_0 stands the applied voltage V at x_0 : e.g. single evoked postsynaptic potential in dendrite; applied voltage by the experimenter upon squid axon; etc.

If we investigate the change of V in a single point from the dendrite (x = 0) we will see that the impulse shrinks or *decrements* with time. So the cable equation becomes reduced to:

$$\tau \frac{\partial V}{\partial t} + V = 0$$

The solution of this differential equation is:

$$V_{(t)} = V_0 \exp\left(-\frac{t}{\tau}\right)$$

or the voltage V drops e = 2,72 times for time τ from the end of applied rectangular impulse V_0.

On space and time, the passive dynamics of an applied potential could be approximated by the following generalized equation:

$$V_{(x,t)} = V_0 \exp\left(-\frac{x}{\lambda}\right)\exp\left(-\frac{t}{\tau}\right)$$

2.1.2 Assessment of the electric field intensity

Knowing the distribution of the voltage V(x,t) spread along the axis of the passive neuronal projection we could find the electric field intensity in space and time after differentiation:

$$\vec{E} = -\nabla V = \frac{dV_{(x,t)}}{dx} = \frac{1}{\lambda} V_0 \exp\left(-\frac{x}{\lambda}\right)\exp\left(-\frac{t}{\tau}\right)$$

where V_0 is the applied voltage at certain point x_0 of the neuronal projection.

2.1.3 Propagation of local electric currents

From the *Ohm's law* we could calculate the *axial current* i_a if we know the applied voltage V upon the dendritic projection:

$$i_a = \frac{\partial V}{\partial l}.\frac{1}{r_i} = \vec{E}\frac{1}{r_i}$$

where l is the direction along the axis of the dendrite. The same equation is valid for the *perimembranous current* i_e outside the dendrite; the only difference is that we should use the r_e value and the current will flow in the opposite direction. The currents flowing along the dendrite under applied depolarizing or hyperpolarizing impulses are known as local currents. *If we have depolarizing impulse there is positive current* $\vec{i}_+$ *flowing from the excited area toward the non-excited regions inside the cytoplasm, while outside of the dendrite the positive currents* $\vec{i}_+$ *flow toward the place of excitation.*

Taking into account that

$$r_i = \frac{4R_A}{\pi d^2}$$

we obtain:

$$i_a = \vec{E}\frac{1}{r_i} = \vec{E}\frac{\pi d^2}{4R_A}$$

The *current density* J through the cross section s of the neuronal projection could be calculated for each point by the differential equation:

$$J = \lim_{\Delta s \to 0} \frac{\Delta i_a}{\Delta s} = \frac{di_a}{ds}$$

or we can find the *mean current density* after integration

$$J_{mean} = \frac{i_a}{s} = \frac{E}{R_A}$$

2.2 Active electric properties – the action potential

If the neuronal projections were absolutely passive then no difference between neurites and ordinary cables would be present. However, as shown by experiment, neurons communicate via non-decrementing electric impulses that propagate with finite velocity varying from 5 to 120 m/s. This implies that the propagation of neuronal impulses (action potentials) relies on a biological process that spends energy and acts in a nonlinear way.

2.2.1 Nernst equation and diffusion potentials

In a *resting neuron* there is a potential difference V = -70 mV between the inner and outer phopsholipid membrane layers. The inner phospholipid layer is negatively charged when compared to the extracellular one. Such membrane potential at rest results from *heterogeneous distribution of ions* – a distribution which therefore differs between the intracellular and extracellular space.

In the late 1880s Walther Nernst, a German chemist, derived an equation that showed the link between the *electric potential* E and the concentration difference of a given ion distributed on the two sides of a membrane (Nernst, 1888; 1889). We refer to E as the *Nernst potential*, the *diffusion potential* or the *equilibrium potential*.

$$E_{ion} = \frac{RT}{FZ} \ln \frac{[Ion]_e}{[Ion]_i}$$

where R is the gas constant (R = 8.31 J.mol^{-1}.K^{-1}), T is the absolute temperature, F is the Faraday's constant (F = 96500 C.mol^{-1}), Z is the valence of the ion, $[Ion]_e$ and $[Ion]_i$ are the ion concentrations in the extracellular and in the intracellular space.

The *Nernst equation* should be understood as follows:

(i) if there is *potential difference* E across the membrane and we have a given ion that can permeate the membrane, after some time a steady equilibrium state will be reached under which no net difference will occur in the flux of the ion across the membrane, though individual ions keep crossing in both directions. With the use of the Nernst equation we can calculate the equilibrium state ratio between the concentrations of the same ion outside and inside the membrane;

(ii) if we have a membrane (not necessarily permeable!) and a given ion that has different concentrations on the two sides of the membrane, we can calculate the potential drop E that will occur due to the unbalanced distribution of the ions at both sides of the membrane.

2.2.2 Resting membrane potential

Knowing the concentrations of K^+ and Na^+ ions inside the cell and in the extracellular matrix allows us to calculate the Nernst potential for those ions. For E_K we obtain a transmembrane voltage of –75 mV, and for E_{Na} we obtain +55 mV. It is easily seen that since in the resting state the membrane potential is –70 mV and it is closer to the Nernst potential of K^+, there will be a weak *electromotive force* of –5 mV pushing potassium ions toward the extracellular space, while for the sodium ions there will be a strong *electromotive force* of +125 mV pushing the sodium ions toward the cellular protoplasm.

It is well known that the membrane potential at rest is kept by the action of the *K^+/Na^+ pump.* It opposes and counteracts to the mentioned electromotive forces above and throws out 3 Na^+ ions – exchanging them for 2 K^+ ions. The active pumping of the K^+/Na^+ pump however spends energy in the form of ATP. That is why the *resting potential* is an "unresting", actively sustained biological state of

the membrane. It therefore is a *unstable state* far from the equilibrium. It gets easily destroyed when the K^+/Na^+ pump is blocked, e.g. by administration of *ouabain*.

2.2.3 Generation of the action potential

The classical experiments with the use of squid axons showed that the action potential is generated via transient increase of the Na^+ conductivity of the membrane, and in some cases increase of Ca^{2+} conductivity. If the rise of the conductivity simply were a transient breakdown in permeability to allow all ions to move across the membrane, it would only depolarize the membrane to zero, not beyond. However the membrane depolarizes reaching +50 mV, whence the mechanism of action potential generation must include *selective increase of conductivity* only of a certain type of ions, e.g. the sodium ones.

Hodgkin & Huxley (1952a, 1952b, 1952c, 1952d, 1952e, 1952f) described the mechanism that produces this inward rush of sodium ions in response to a small depolarization of the squid axonal membrane. After applying a brief depolarizing impulse above certain threshold value, the *voltage-gated sodium channels* open. The energy for it is provided by the *electrochemical gradient* of Na^+ across the membrane, according to the principles already outlined above. The explosive nature of the flow of Na^+ ions, triggered by an initial, small depolarization of the membrane, is due to the voltage-sensitive properties of the Na^+ channel protein. A *positive feedback* loop process is started.

When the membrane begins depolarizing, it causes the Na^+ conductance to start an increase that depolarizes the membrane further. This in turn increases the Na^+ conductance, … and so on. This is the kind of *self-reinforcing regenerative relation* that characterizes various kinds of devices; a similar relation between heat and chemical reaction, for example, underlies the explosion of gunpowder (Shepherd, 1994). One can say that it is the property that puts the "action" into the action potential. It gives the impulse a threshold, below which it fails to fire, above which it is fully successful: one thus says that it is "all-or-nothing".

The successful transmission of information along the axon, nevertheless, requires inactivation of the voltage-gated sodium channels at a certain step. Otherwise the whole membrane would be depolarized, until it reaches about +50 mV inside and it settles in this excited state. If it were the case, no subsequent information

could be transmitted. Actually the voltage-gated sodium channels get inactivated when the membrane potential reaches +40 mV, preventing such situation.

Another important biological consequence of the sodium channel inactivation is the interposition of a *refractory period* during which any potential applied, even over the threshold, does not initiate any action potential. The existence of a refractory period allows the action potential to propagate along the axon without re-exciting another action potential. Concurrent with the sodium channel inactivation a further important process is started – *voltage-gated K^+ channels* do open and quickly restore the resting membrane potential, even slightly overcompensating it, a process known as *hyperpolarization*.

The interplay of voltage-gated (i) *sodium inward rush*, (ii) *sodium channel inactivation* and (iii) *potassium efflux shifted in time* allows the neurons generate action potentials that propagate in one direction in the form of *solitary waves*. The propagation of the action potentials is different in unmyelinated axons, myelinated axons and dendrites.

2.2.3.1 Action potential in unmyelinated axons

In an unmyelinated axon the action potential propagates in the form of a *solitary wave*. If about the midpoint of a lengthy squid axon a brief depolarization is applied, it propagates in both directions, because in both directions the sodium channels stand in a resting state. If the action potential however is generated in vivo at the axonal hillock in most cases the action potential propagates down the axon and cannot return back, because the voltage-gated sodium channels switch off into a refractory state soon after a peak membrane depolarization is reached. (We will see in the next sections that exceptions from this rule are also known because the dendrites and soma do possess various types of voltage gated ion channels).

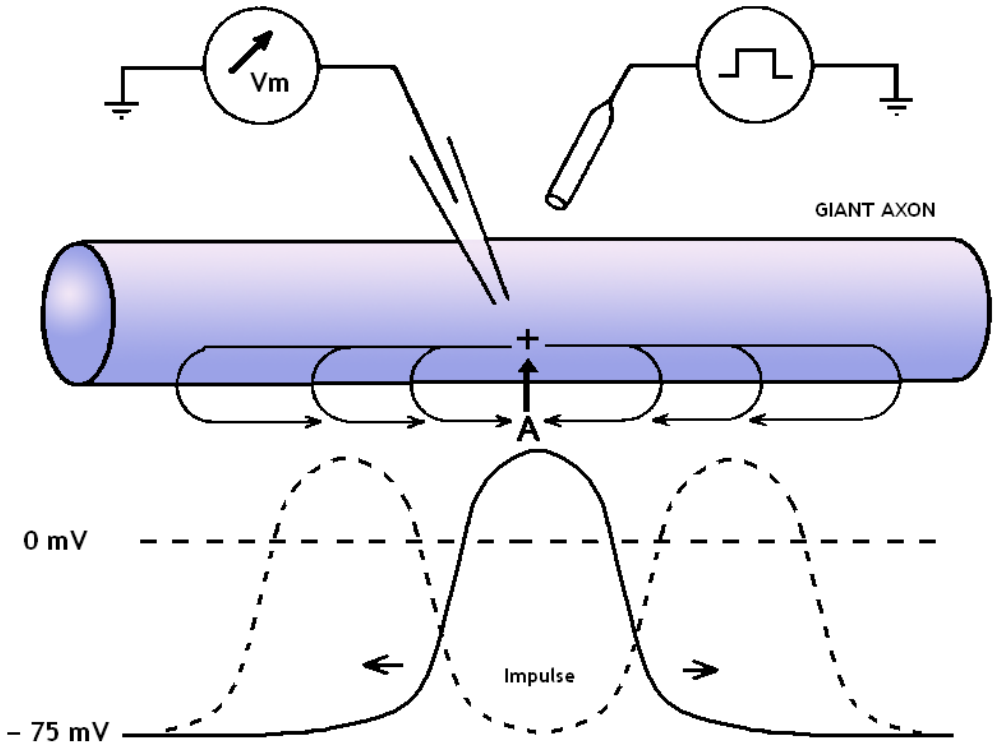

FIG 6 The impulse in the squid axon. The impulse has been triggered by a brief depolarization at A. Note that the impulse has the ability to spread in both directions when elicited experimentally in the middle of a nerve.

2.2.3.2 Action potential in myelinated axons

The diameter of axons varies from 1μm to 25 μm in humans. Axons with small diameter could be non-myelinated. However the larger axons are ensheathed by multiple membrane layers known as *myelin*. In the *central nervous system* (CNS) the myelin is produced by supportive glial cells called *oligodendrocytes*. The oligodendrocytic membrane rotates around the axon and forms a multiple-layered phospholipid structure that insulates the axon from the surrounding environment. One axon is insulated by numerous oligodendrocytes abreast, each ensheating a short segment only. Yet between two successive oligodendrocytes tiny places remain where the axonal membrane is non-myelinated. Between the embracing membranes of different oligodendrocytes, therefore, the axonal membrane presents such places free of myelin. They are called *nodes of Ranvier* and are enriched in voltage-gated ion channels.

In the *peripheral nervous system* (PNS) the myelin is produced not by oligodendrocytes but by *Schwann cells*. The main principles governing the electric behavior of axons however remain the same.

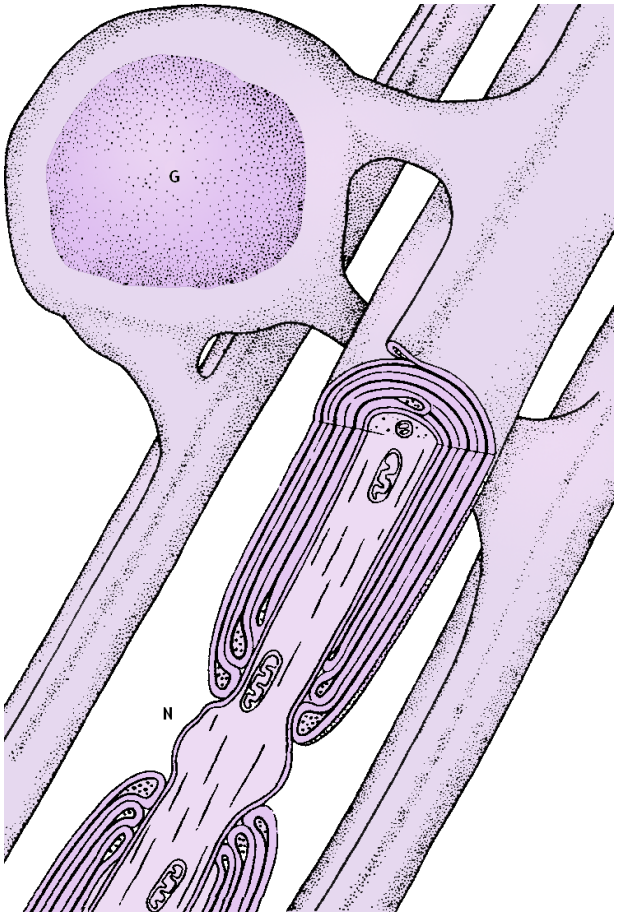

FIG 7 Oligodendrocytic glial projections wrap three axons in CNS forming multilamelar myelin envelopes. One oligodendrocyte typically supports 30-40 myelinated segments of different axons in the way indicated on the diagram. Legend: G, oligodendrocytic glial cell; N, node of Ranvier.

In the *myelinated axons* the membrane conductivity for ions is substantially decreased by the multiple glial wrappings around the axon in the form of myelin. Since the myelin sheath is not permeable for ions, the ion leakage across the membrane is prevented and thus the axonal space constant λ is increased. The increment of λ means that the passive spread of voltage along the axon does not decrement so fast – and the length of axon in which the voltage stands over the threshold is greater. This allows farther parts of axonal membrane to become activated, thereby increasing the conducting velocity of the action potential. In the myelinated axons the *spike* (action potential) does not propagate smoothly, therefore: it jumps from node to node of Ranvier. This is why the propagation of the action potential is called *saltatory conduction*.

Saltatory conduction is made very effective and economic because the sodium and potassium channels are clustered at the Ranvier nodes only. This allows such neurons, possessed with less synthesized proteins (ion channels) but more properly distributed, to achieve effective communication via electric signals. On the other hand the passive spread of voltage remains several orders of magnitude faster that the conducting velocity of the action potential; myelinated neurons wisely invented the mechanism to increase the conducting velocity of axonal spikes by way of increasing λ – allowing only passive electric processes in the regions between two Ranvier nodes.

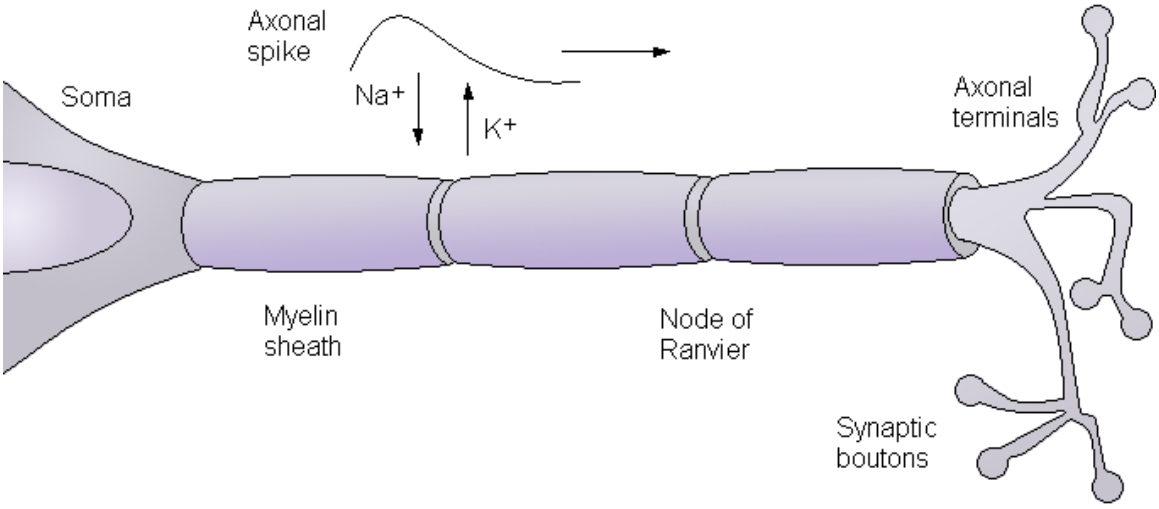

FIG 8 Axonal spike in myelinated neuron generated by sodium and potassium ion currents across the membrane in the nodes of Ranvier.

Higher stimulus intensity upon the nerve cell is thus reflected in *increased frequency* of impulses, not in higher voltages because all action potentials look essentially the same. The speed of propagation of the action potential for mammalian motor neurons is 10-120 m/s; while for unmyelinated sensory neurons it's about 5-25 m/s. (Unmyelinated neurons fire in a continuous fashion, i.e. without the jumps, but the ion leakage slows the rate of propagation).

2.2.3.3 Active processes in 'hot spots' of dendrites

Usually one thinks that in dendrites the passive spread of voltage is the only mechanism that allows for effective dendritic computation. Experimental evidence disproves this common belief. Molecular studies via different types of labeling procedures have indeed shown that dendrites posses voltage-gated ion channels, and that these channels are located in domains – the so-called *"hot spots"*.

Although the dendritic membrane is unmyelinated, the ion channel distribution on it is inhomogeneous. The dendritic ion channels are clustered at (i) the postsynaptic membrane, (ii) the dendritic spine heads and (iii) the places of dendritic branching. This particular clustering is supported by anchoring of the voltage gated ion channels to components of the cytoskeleton and also by incorporating the ion channels into *rigid* highly specialized domains of the membrane, known as *lipid rafts*.

Lipid rafts are subdomains of the plasma membrane that contain high concentrations of *cholesterol* and *glycosphingolipids*. While the rafts exhibit a distinctive protein and lipid composition differing from the rest of the membrane, all rafts do not appear to be identical in terms of the proteins or the lipids that they contain. Indeed several types of lipid rafts were found to exist, some of which are highly specific for neurons. It thus seems that lipid rafts introduce order in the membrane, which initially was thought as if it were highly fluid and chaotic (Linda J. Pike, 2003). Recent advances in lipidology show both heterogeneity of the membrane component distribution as well as the formation of organized membrane domains in the form of rafts. As considered below, the clustering of voltage gated ion channels and their heterogeneous distribution allow dendrites to implement different computational gates such as AND, OR, and NOT.

The next diagram summarizes the three types of active spread of potentials: (i) in unmyelinated axons, (ii) in myelinated axons and (iii) in dendritic trees.

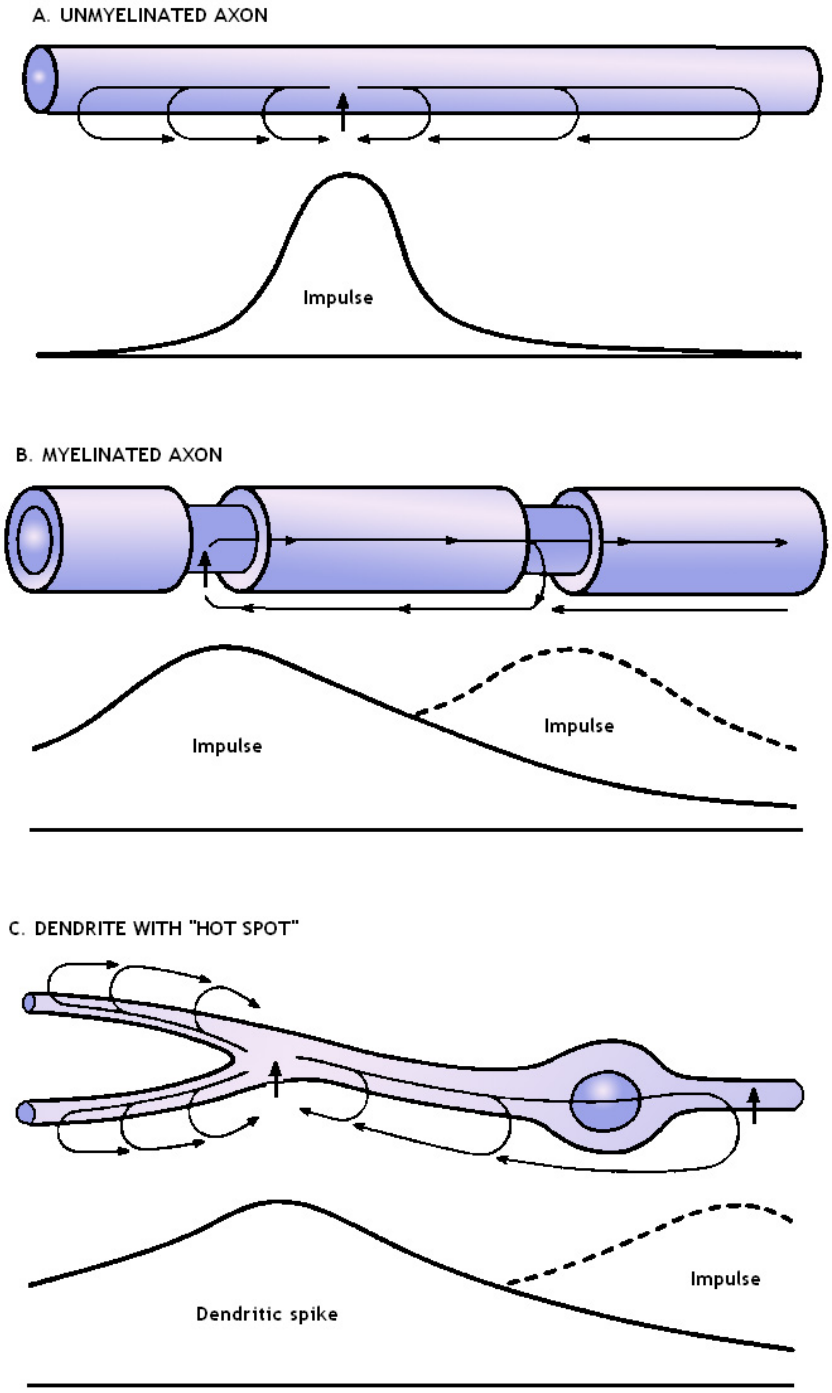

FIG 9 Comparative image of the mechanisms for spread of the impulse. A. Continuous conduction in an unmyelinated axon. Amplitude scale is in millivolts. B. Discontinuous (saltatory) conduction from node to node in a myelinated axon. C. Discontinuous spread from "hot spot" to "hot spot" in a dendrite. In all diagrams, the impulses are shown in their spatial extent along the fiber at an instant of time. The extent of current spread is governed by the cable properties of the fiber.

2.3 Dendrites

The main communication between two neurons is achieved via axo-dendritic synapses located at the top of the *dendritic spines* that are typical for the cortical neurons. It is known that the dendritic postsynaptic membranes convert the neuromediator signal into postsynaptic electric current. The neuromediator molecules bind to specific postsynaptic ion channels and open their gates. The ion species that enter the dendritic cytoplasm then change the membrane potential.

In this section we will calculate the electric intensity $\vec{E}$ in the dendritic protoplasm as well as the magnetic flux density $\vec{B}$ born by the cytoplasmatic electric currents. In our calculations we will consider only the postsynaptic potentials evoked by a neurotransmitter and will use the passive cable equation for dendrites. However we should remember that

(i) the action potentials generated at the axonal hillock exhibit passive electric properties and lead to a decrementing in space-time, retrograde (also called antidromic) rise of the electric field in the basal dendrites and the neuronal soma;

(ii) some action potentials generated at the axonal hillock propagate retrogradely, because of the voltage gated sodium and calcium channels in dendrites.

2.3.1 Electric intensity in dendritic cytoplasm

Sayer et al. (1990) measured the evoked excitatory postsynaptic potentials (EPSP) by single firing of the presynaptic terminal. In their study 71 unitary EPSPs evoked in CA1 pyramidal neurons (CA means Cornus Ammonis, or hippocampus) by activation of single CA3 pyramidal neurons were recorded. The peak amplitudes of these EPSPs ranged from 0.03 to 0.665 mV with a mean of 0.131 mV. Recently it become clear that the remote synapses produce higher EPSPs or in other words they "speak louder" than the proximal synapses because of voltage-gated sodium channel boosting (Spruston, 2000) – so that the somatic EPSP amplitude is independent of synapse location in hippocampal pyramidal neurons (Magee & Cook, 2000). In the calculations carried out in this paper we will consider that the single EPSP magnitude is 0.2mV (London & Segev, 2001).

Before we calculate the electric field intensity $\vec{E}$ in the dendritic cytoplasm we should assess the values of the time and space constants in the cable equation.

In vivo the *time constant* τ depends on the membrane resistance R_m. It changes in time because the membrane channels close and open; i.e. in vivo the membrane is active, not a passive device. It was experimentally shown that the resistivity of the dendritic membrane follows a sigmoid function (Waldrop & Glantz, 1985). Its time constant τ depends on the channel conductances (Mayer & Vyklicky, 1989) and if directly calculated we obtain a wide range of results, from 10 ms to 100 ms. The change in time of the electric properties of neuronal membranes leads to a non-linear behavior of the neuronal projections – and as we saw because these processes must be fueled with energy they are labelled as *active processes*. All these things considered, if interested in the passive membrane properties we could approximate τ as constant in time and take τ = 30 ms.

The *space constant* λ depends on the geometry of the neuronal projection and particularly on its diameter. The space constant λ for a dendrite with d = 1μm is:

$$\lambda = \sqrt{\frac{dR_M}{4R_A}} = \sqrt{\frac{10^{-6} m \times 0.5\Omega.m^2}{4 \times 1\Omega.m}} \approx 353\mu m$$

Here it should be mentioned that the space constant λ depends on the dendrite's diameter. So in order to be more precise in our calculations we must decompose the dendritic tree into smaller segments with approximately the same λ (Sajda, 2002).

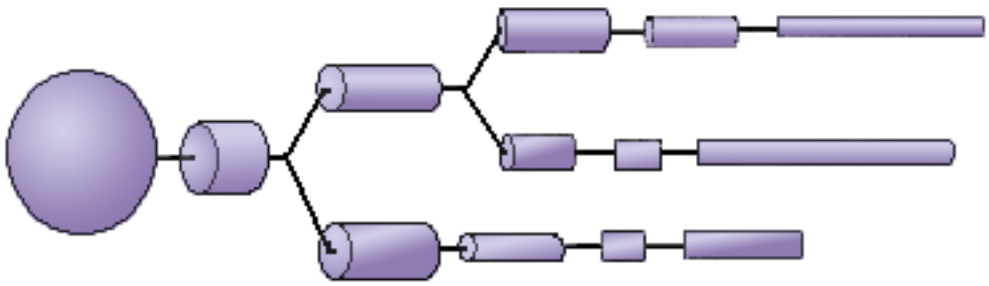

FIG 10 Cable net approximation of the dendritic tree.

But if we need only a rough approximation we could consider that the dendrite has a constant diameter of 1μm and we can use the calculated value for the space constant, namely putting λ = 353 μm.

On the graphics below it is presented the distribution in space and time of a single EPSP with magnitude 0.2mV applied at the top of such dendritic projection.

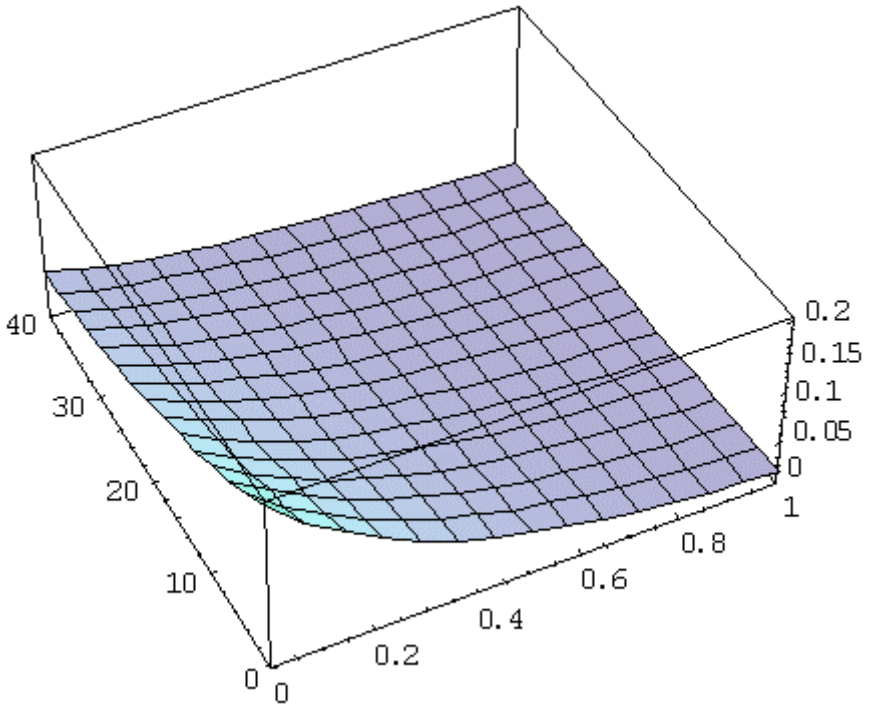

FIG 11 Spatio-temporal decrement of a single EPSP in time interval of 40 ms in dendrite with diameter d = 1 μm, length l = 1 mm, space constant λ = 353 μm and time constant τ = 30 ms.

The maximal electric field intensity for a single excitatory postsynaptic potential with magnitude 0.2 mV is $\vec{E}$ = 0.57 V/m.

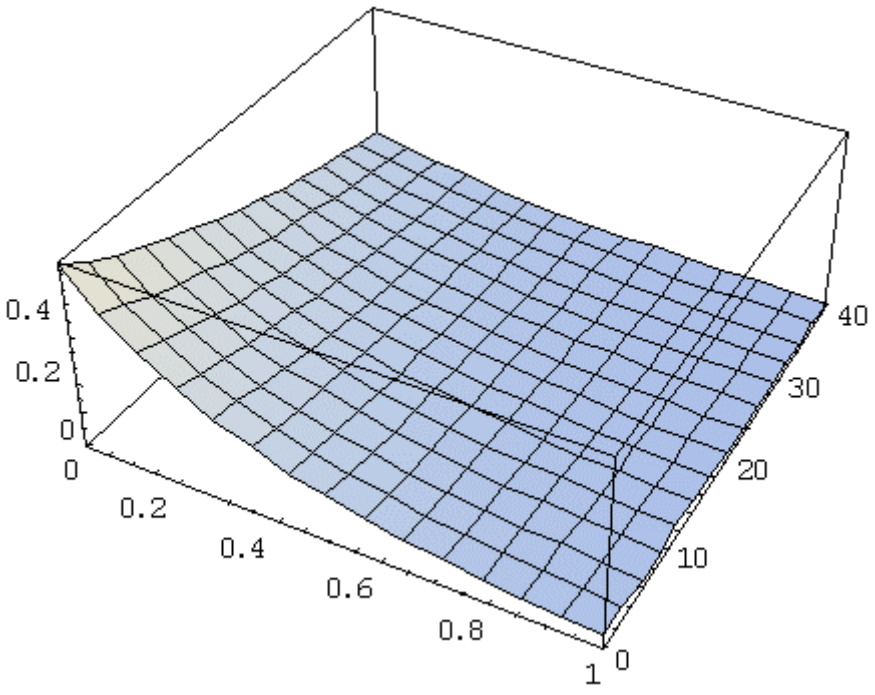

FIG 12 (Previous page) Distribution of the electric intensity along the axis of the dendrite after application of single EPSP with magnitude of 0.2 mV at the top of a single dendrite with diameter d = 1 μm, length l = 1 mm, time interval of 40 ms, λ = 353 μm and τ = 30 ms.

Considering that the excitatory postsynaptic potentials (EPSPs) and the inhibitory postsynaptic potentials (IPSPs) could summate over space and time, it is not a surprise that, in case of multiple dendritic inputs, the measured axial dendritic voltages reach tens of millivolts. If 300 or 400 EPSPs get temporally and spatially summated, the electric intensity along the dendritic axis could thus be as high as 10 V/m in different regions of the dendritic tree. The accuracy of our calculations is supported by Jaffe & Nuccitelli (1977) who estimate the intracellular electric fields in vivo to have intensity of 1-10 V/m.

2.3.2 Electric currents in dendrites

Calculation of *electric current* along the dendrite after an EPSP with magnitude of 0.2 mV gives us:

$$i_a = \vec{E}\frac{\pi d^2}{4R_A} = \frac{0.57V.m^{-1} \times 3.14 \times 10^{-12} m^2}{4 \times 1\Omega m} \approx 0.45 pA$$

This result is smaller than the registered evoked inhibitory postsynaptic currents (eIPSCs), whose amplitude varies from 20 pA to 100 pA (Kirischuk et al., 1999; Akaike et al., 2002; Akaike & Moorhouse, 2003).

The mean current density J through the cross section of the neuronal projection could be calculated from:

$$J_{mean} = \frac{i_a}{s} = \frac{E}{R_A} = \frac{0.57V.m^{-1}}{1\Omega m} = 0.57 A/m^2$$

The above calculation is valid for a single EPSP with amplitude of 0.2 mV. We should remind, too, that it yields *mean current density* (i.e. averaged one) since the current density decrements in space exactly as the voltage does.

2.3.3 Magnetic flux density in dendritic cytoplasm

The distribution of the magnetic intensity $\vec{H}$ inside the projection (cable) and outside it offers a different picture. This is so because inside the cable $\vec{H}$

depends on the *partial interweaved current* i_x, while outside the cable the whole current is already inside the $\vec{H}$ loop. The magnetic intensity $\vec{H}$ outside the cable is

$$\vec{H} = \frac{i}{2\pi x}$$

where i is the *current* in the cable and x is the *distance* from the axis of the cable.

The magnetic intensity inside the cable depends on the *partial interweaved current* i_x, so in case with constant current density J we can write

$$\vec{H} = \frac{i_x}{2\pi x} = J\frac{x}{2}$$

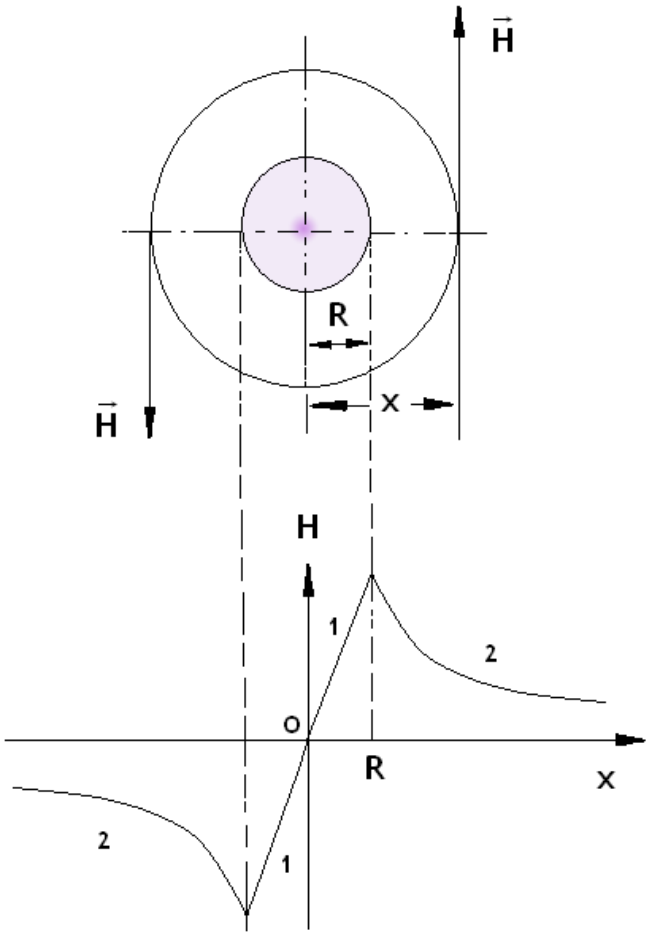

FIG 13 Transversal slice of a cable with radius R and distribution of the magnetic intensity inside the cable and outside it. Legend: H, magnetic intensity; R, cable radius; 1, area inside the cable; 2, area outside the cable; x, distance from the cable axis. Modified from Zlatev (1972).

The current inside dendrites is experimentally measured to be from 20 pA to 100 pA for GABAergic synapses (Akaike & Moorhouse, 2003). Using the formula:

$$\oint_{\Gamma} \vec{H} \cdot d\vec{l} = i$$

we can find the magnetic intensity for a contour Γ with length l = πd that interweaves the whole current i_a. For dendrite with d = 1μm we obtain:

$$H = \frac{10^2 \times 10^{-12} A}{3.14 \times 10^{-6} m} = 3.18 \times 10^{-5} A/m$$

If we consider that the water and the microtubules form a system augmenting the magnetic strength known as *ferrofluid* (Frick et al., 2003; Ávila & Funes, 1980) then in the best-case with effective magnetic permeability $\mu_{eff} \sim 10$, where

$$\mu_{eff} = \frac{\mu}{\mu_0}$$

we will obtain the maximal possible magnitude of the magnetic flux density $\vec{B}$ inside the neuronal projection:

$$\vec{B} = \mu_{eff} \mu_0 \vec{H}$$

$$B = 10 \times 4\pi \times 10^{-7} H.m^{-1} \times 3.18 \times 10^{-5} A.m^{-1} \approx 4 \times 10^{-10} T$$

We should warn however that this maximal magnetic flux density $\vec{B}$ is just beneath the dendritic membrane, and in a point of the dendritic axis the magnetic flux density is average on the biologically relevant scales is *zero*. On microphysical scales it is not zero, of course; the quantum vacuum's "popping out" of photons generates huge yet quasi-local values.

The *Earth's magnetic field* is on the order of ½ Gauss (5×10^{-5} T). *Gauss* is a unit used for small fields like the Earth's magnetic field and 1 Gauss is 10^{-4} T. It is thus obvious that the magnetic field generated by the dendritic currents cannot be used as informational signal because the noise resulting from the Earth's magnetic field will suffocate it (Georgiev, 2003). *Or in other words any putative magnetic signal inside the neuronal network will be like a "butterfly in a*

hurricane". This is why the magnetic field cannot encode information and be used in the informational processing performed by neurons.

2.3.4 Active dendritic properties

After the neuromediator molecules bind to postsynaptic ion channel receptors, the latter open their pores. A flux of ions is thus usually triggered across the membrane. The translocation of these ions changes the transmembrane potential, V, and the applied voltage V spreads passively toward the spine stalk, nearby spines and the supporting dendrite. Biological data however show that both the spine heads as well as the *"hot spots"* or patches of the dendritic membranes enriched with voltage sensitive channels, can amplify or process the postsynaptic potentials (PSPs) via non-linear response.

2.3.4.1 Amplification of synaptic inputs

In an intracellular study of hippocampal neurons Spencer & Kandel (1961) described *fast prepotentials* (FPPs), small potential steps immediately preceding full-blown spikes. They concluded that the FPPs were also spikes because of their all-or-none character and because their repolarization was faster than the membrane time constant. In their discussion, Spencer & Kandel (1961) proposed that FPPs were *distant dendritic spikes* produced in a "trigger zone," presumably associated with a bifurcation of the apical dendrite. Although conceptually influential, prepotentials did not furnish unambiguous experimental evidence for active dendrites (Yuste & Tank, 1996). Nevertheless, in a series of seminal papers Llinas and collaborators ushered in a new era in dendritic physiology by recording intracellularly from dendrites of Purkinje neurons, directly demonstrating the existence of *dendritic spikes* (Llinas & Nicholson, 1971; Llinas & Hess, 1976; Llinas & Sugimori, 1980).

The *dendritic spine* consists of a *spine head* (where the synapse gets formed) and *spine stalk* (a narrowing of the spine diameter that raises the stalk resistance up to 800 MΩ (Miller et al., 1985). Based upon the assumption that spine head membrane is passive, previous studies concluded that the efficacy of a synapse onto a spine head would be less than or equal to the efficacy of an identical synapse directly onto the *"parent" dendrite* (Chang, 1952; Diamond et al., 1970; Coss & Globus, 1978). However, for an *active spine head* membrane, early steady state considerations suggested that spines might act as synaptic amplifiers (Miller

et al., 1985). This means that the ion channels located in the spine head are voltage-gated and the EPSP propagation will exhibit non-linear properties. When the voltage in the spine reaches certain voltage magnitude (threshold) the channels open and amplify the synaptic input.

2.3.4.2 Implementation of classical computational gates in dendrites

In the cerebral cortex, about 90% of the synapses are on spines of dendritic trunks and branches. It thus may be assumed that the dendritic microcircuits provide the main substrate for synaptic interactions. Since much of this dendritic substrate is remote from the cell body, our knowledge of the basic properties involved is limited. Information, nonetheless, has been obtained by recording intracellularly from dendrites in isolated cortical slices (Shepherd, 1994). These experiments supported previous evidence suggesting that the cortical dendrites, like those of many other types of neurons, harbor ionic membrane channels that are *voltage sensitive*. It has been believed that these sites are located at the branch points, where they would serve to *boost* the responses of distal dendrites.

The ubiquitousness of voltage-dependent channels suggested that they may also be present in spines. The way that their presence would contribute to spine responses and spine interactions has been explored in computer simulations. A simulation consists in representing some portion of a dendritic tree with its spines by means of a system of compartments – each compartment comprising the electrical properties of a dendritic segment or spine. It was shown that an active response in a spine would indeed boost the amplitude of the synaptic response spreading out of the spine. It was further shown that the current spreading passively out of one spine readily enters neighboring spines, where in turn it can trigger further active responses. In this way, it is thought, distal responses can be brought much closer to the cell body by a process resembling saltatory conduction in axons.

A third interesting property is that the interactions between active spines can be readily characterized in terms of *logic operations* (Shepherd & Brayton, 1987). Thus, an AND operation is performed when two spines must be synaptically activated simultaneously in order to generate spine responses. An OR operation is performed when either one spine or another can be activated by a synaptic input. Finally, a NOT-AND operation occurs when a response can be generated by an excitatory synapse if an inhibitory synapse is simultaneously active. The interest

of these simulations is that these three logic operations, together with a level of background activity, are sufficient for building a computer.

This result of course does not mean that the cortex is a computer; rather, it helps to define more clearly the nature of the synaptic interactions that take place at the microcircuit level. Defining these interactions more clearly is a step toward identifying the basic operations underlying the higher levels functions of circuit organization. One can speculate that interactions of this nature within dendrites may serve the bodily operations at play both in our outer behavior and higher cognitive functions such as logical and abstract reasoning.

2.3.4.3 Mapping of voltage gated ion channels in dendrites

In the last several years there was extensive study of dendritic spine active properties and a lot of experiments mapped the distribution of the *voltage-gated ion channels*. At the present time it seems that cortical neurons are the best candidates for neurons performing active computation at the level of dendritic spines. On the next table we present the specific distribution of voltage gated ion channels in the apical and basal dendrites of a typical cortical neuron - the hippocampal CA1 neuron.

Table 3 Distribution of ion channels in the dendritic tree of a CA1 hippocampal neuron. Data obtained by Neuron DB. The channel names are updated according to The IUPHAR Compendium of Voltage-gated Ion Channels released in 2002.

Distal apical dendrite	Middle apical dendrite	Proximal apical dendrite	Distal basal dendrite	Middle basal dendrite	Proximal basal dendrite
$Ca_v2.2$	$Ca_v2.2$	$K_v1.1$ $K_v1.2$ $K_v1.6$	$K_{Ca}1.1$ $K_{Ca}2.1$ $K_{Ca}2.2$	$Na_v1.x$	$Na_v1.x$
$K_v3.3$ $K_v3.4$ $K_v4.1$ $K_v4.2$ $K_v4.3$	$K_v1.1$ $K_v1.2$ $K_v1.6$	$Na_v1.x$			
$Ca_v2.1$ $Ca_v2.3$	$Ca_v2.1$ $Ca_v2.3$	$Ca_v2.1$ $Ca_v2.3$			
$Ca_v3.1$ $Ca_v3.2$ $Ca_v3.3$	$Na_v1.x$	$Ca_v3.1$ $Ca_v3.2$ $Ca_v3.3$			
$Na_v1.x$	$Ca_v3.1$ $Ca_v3.2$ $Ca_v3.3$	$Ca_v1.2$ $Ca_v1.3$			
$Ca_v1.2$ $Ca_v1.3$	$Ca_v1.2$ $Ca_v1.3$	$Ca_v2.2$			
HCN1 HCN2 HCN3	$K_v3.3$ $K_v3.4$ $K_v4.1$ $K_v4.2$ $K_v4.3$	$K_v3.3$ $K_v3.4$ $K_v4.1$ $K_v4.2$ $K_v4.3$			
	HCN1 HCN2 HCN3	HCN1 HCN2 HCN3			

According to the IUPHAR nomenclature the name of an individual channel consists of the chemical symbol of the principal permeating ion (e.g. Na) with the principal physiological regulator (e.g. voltage) indicated as a subscript (e.g. Na_v). The number following the subscript indicates the gene subfamily (e.g. Na_v1), and the number following the full point identifies the specific channel isoform (e.g. $Na_v1.1$). This last number has been assigned according to the approximate order in which each gene was identified. Splice variants of each family member are identified by lower-case letters following the numbers (e.g. $Na_v1.1a$).

2.3.4.3.1 $Na_v1.x$ channels

The abbreviation $Na_v1.x$ denotes all nine types of voltage gated sodium channels from $Na_v1.1$ to $Na_v1.9$. Sodium impulses may underly fast prepotentials that boost distal EPSPs. Lipowsky et al. (1996) experimentally verified that the dendritic Na^+ channels amplify EPSPs in hippocampal CA1 pyramidal cells. Na^+

action potentials support backpropagating impulses and can activate Ca^{2+} action potentials (Spruston et al., 1995). Patch recordings yield an approximate channel density of 28 pS/micron^2 in juvenile rats, which were 4 weeks of age, rising to 61 pS/micron^2 in older rats. Channel density was similar in other dendritic compartments (Magee & Johnston, 1995; Tsubokawa et al., 2000). Caldwell et al. (2000) showed with immunofluorescent mapping that $Na_v1.6$ channels are localized not only in axons and nodes of Ranvier but also in dendrites of cortical neurons.

Recordings using the intracellular perfusion method showed no differences between the I-V characteristics of CA1 and CA3 neurones for this current. In contrast to this, the steady-state inactivation of both types of neurones was significantly different (Steinhauser et al., 1990). Inactivation of the dendritic Na^+ channel contributes to the attenuation of activity-dependent backpropagation of action potentials (Jung et al., 1997). Slow inactivation of sodium channels in dendrites and soma will modulate neuronal excitability in a way that depends, in a complicated manner, on the resting potential and previous history of action potential firing (Mickus et al., 1999). Dendrites can fire sodium spikes that can precede somatic action potentials, the probability and amplitude of which depend on previous synaptic and firing history. Some dendritic spikes could occur in the absence of somatic action potentials, indicating that their propagation to soma is unreliable (Golding & Spruston, 1998). Single action potential backpropagations show a dichotomy of either strong attenuation (26-42%) or weak attenuation (71-87%). The dichotomy seems primarily conferred by differences in distribution and density of the voltage dependent sodium and potassium channel (A-type, especially) along the somatodendritic axis (Golding et al., 2001).

2.3.4.3.2 $Ca_v1.2$ and $Ca_v1.3$ channels

These two channels are also known as L-type Ca^{2+} channels or high voltage-activated, large conductance (HVA1) channels. Using a monoclonal antibody Westenbroek et al., (1990) showed that the proximal dendrites and somata of hippocampal neurons label for L-type Ca^{2+} channels and that these channels tend to cluster near the bases of the neural processes. In dendrite-attached patch-clamp recordings L-type channels were occasionally encountered primarily in the more proximal dendrites – and in the soma (Magee & Johnston, 1995). Ca^{2+} fluorescence imaging shows that application of L-channel antagonists reduces the Ca^{2+} influx associated with backpropagating action potentials, and has a

significantly greater effect in the proximal dendrites than in more distal dendrites (Christie, 1995).

2.3.4.3.3 $Ca_v2.1$ and $Ca_v2.3$ channels

$Ca_v2.1$ is known as P/Q-type Ca^{2+} channel and Cav2.3 as R-type Ca^{2+} channel. Dendrite-attached patch-clamp techniques from the apical dendrites (up to 350 µm away from soma) of CA1 pyramidal neurons in rat hippocampal slices indicate channels similar in their basic characteristics to one or more of the high voltage-activated, moderate conductance (HVAm) channel types (most likely P/Q- or R-type channels)(Magee & Johnston, 1995). Ca^{2+} fluorescence imaging shows that application of P-channel antagonists reduces the Ca^{2+} influx associated with backpropagating action potentials. Action potential-mediated depolarization can result in the elevation of dendritic intracellular Ca^{2+} concentration (Jaffe, D.B. et al, 1992), which is important for the induction of long-term changes in synaptic strength (Spruston et al., 1995).

2.3.4.3.4 $Ca_v2.2$ channels

Also known as N-type Ca^{2+} channels. Ca^{2+} fluorescence imaging shows that application of N-channel antagonists slightly reduces the Ca^{2+} influx associated with backpropagating action potentials (Christie, 1995). With the use of confocal microscopy these channels were found to be localized on the soma, dendrites, and a subpopulation of dendritic spines (Mills et al., 1994).

2.3.4.3.5 $Ca_v3.1$, $Ca_v3.2$ and $Ca_v3.3$ channels

These 3 channels are also known as T-type Ca^{2+} channels. Patch recordings yield in dendrites an approximate channel density of 7 pS/micron^2 in juvenile rats, which were 4 weeks of age – rising to 10 pS/micron^2 in older rats. T-type channels are less dense in the soma than in the dendrites (Magee & Johnston, 1995). Ca^{2+} channel density was similar in other dendritic compartments, and in general lower than Na^+ channel density (Magee & Johnston, 1995). However, in a few apical patches the channel density was increased three-fold, which could indicate *channel clustering*. Ca^{2+} fluorescence imaging shows that application of T-channel antagonists reduces the Ca^{2+} influx associated with backpropagating action potentials, and has a twofold greater effect in the soma than in the dendrites (Christie, 1995).

2.3.4.3.6 $K_v1.1$, $K_v1.2$ and $K_v1.6$ channels

These channels are also known as delayed rectifiers or D-type K^+ channels, because are sensitive to dendrotoxin (DTX). A D-type potassium current is involved in dendritic calcium spikes initiation and repolarization (Golding et al, 1999).

2.3.4.3.7 $K_v3.3$, $K_v3.4$, $K_v4.1$, $K_v4.2$ and $K_v4.3$ channels

These channels, also called A-type K^+ channels, are responsible for the I_A current. Patch-clamp recordings reveal a high density of A-type K^+ channels in the dendritic tree, which increases with the distance from the soma (Hoffman et al., 1997). A shift toward more depolarized potentials of the activation curve has also been observed in mid and distal dendrites (more than 100µm) (Hoffman et al., 1997). These channels prevent initiation of an action potential in the dendrites, limit the backpropagation of action potentials into the dendrites, and reduce excitatory synaptic events (Hoffman et al., 1997). Single action potential backpropagations show a dichotomy of either strong attenuation (26-42%) or weak attenuation (71-87%). The dichotomy seems to be primarily conferred by differences in distribution, density, etc. of voltage dependent sodium and potassium channel (A-type, especially) along the somatodendritic axis (Golding et al., 2001). In the hippocampus, CA1 neurons and subicular neurons differ in firing pattern (the former being regular and the later being either regular, weakly bursting or strongly bursting) and resting membrane properties (such as input resistance and membrane time constant); however, in both regions a low concentration of 4-AP can convert neurons into firing bursting action potentials (Staff et al., 2000).

2.3.4.3.8 $K_{Ca}1.1$, $K_{Ca}2.1$ and $K_{Ca}2.2$ channels

$K_{Ca}1.1$ is known as BK channel, $K_{Ca}2.1$ is known as SK1 channel and $K_{Ca}2.2$ as SK2 channel. A single-electrode voltage-clamp technique was employed on slices to examine slow after-hyperpolarization (sAHP). This was achieved by using conventional procedures to evoke an after-hyperpolarization (AHP) in the current clamp, rapidly followed by a switch into voltage clamp (hybrid clamp). The AHP current showed a dependence on extracellular K^+ close to that predicted by the Nernst equation. It could be blocked by Cd^{2+} or norepinephrine and showed a requirement for voltage-dependent Ca^{2+} entry, but did not show any clear intrinsic voltage dependence. Once activated, AHP current is not turned off by

hyperpolarizing the membrane potential (Lancaster & Adams, 1986). Cell-attached patches on the proximal 100 µm of the apical dendrite did not contain sAHP channels. Amputation of the apical dendrite approximately 30 µm from the soma, while simultaneously recording the slow AHP whole cell current at the soma, depressed the sAHP amplitude by only approximately 30% compared with controls. Somatic cell-attached and nucleated patches did not contain sAHP current. Amputation of the axon about 20 µm from the soma had little effect on the amplitude of the slow AHP. By this process of elimination, it is suggested that the sAHP channels may be concentrated in the basal dendrites of CA1 pyramids (Bekkers, 2000).

In situ hybridization showed high levels of expression of SK1 and SK2 channels in CA1-3 regions of the hippocampus (Stocker & Pedarzani, 2000). The role of large-conductance Ca^{2+}-dependent K^+ channels (BK) in spike broadening during repetitive firing was studied by using sharp electrodes and by computer modelling. The amplitude of the fast after-hyperpolarization (fAHP) rapidly declined during each train. Suppression of BK-channel activity with the selective BK-channel blocker iberiotoxin, the non-peptidergic BK-channel blocker paxilline, or calcium-free medium, broadened the first spike to a similar degree, of approximately 60 %. (Shao, L.R. et al., 1999).

2.3.4.3.9 HCN1, HCN2 and HCN3 channels

These channels, also called hyperpolarization-activated, cyclic nucleotide-gated cation channels, are responsible for the Ih current. A depolarizing lag during larger hyperpolarizing voltage transients is indicative of Ih current in CA1 pyramidal neurons (Spruston & Johnston, 1992). Membrane patches recorded in the cell-attached patch configuration from the soma and apical dendrites revealed an Ih that increased over six-fold from soma to distal dendrites. Ih demonstrated a mixed Na^+-K^+ conductance and was sensitive to low concentrations of external CsCl. As a result of Ih the propagation of subthreshold voltage transients is directionally specific. The elevated dendritic Ih density decreases EPSP amplitude and duration and reduces the time window over which temporal summation takes place (Magee, 1999).

2.4 Neuronal somata

From the computational point of view, the neuronal soma integrates the inputs from the dendrites. The passive properties of dendrites lead to decrement of the

EPSPs and IPSPs that reach the soma. This however allows for the EPSPs and IPSPs to summate over space and time – and when a critical threshold in the soma is reached a non-decrementing axonal spike to occur.

The nonlinear properties of the neuronal output are due to voltage-gated Na^+ channels located at the axon hillock that exhibit positive feedback. When a critical threshold of the transmembrane voltage of about -55mV is reached in the *axonal hillock,* more and more voltage gated sodium ion channels get open and an action potential is triggered. The magnetic and the electric field strengths are expected to be the same as in the axon, with maximal magnetic strength of 10^{-7} T and maximal electric strength of 10 V/m (see below).

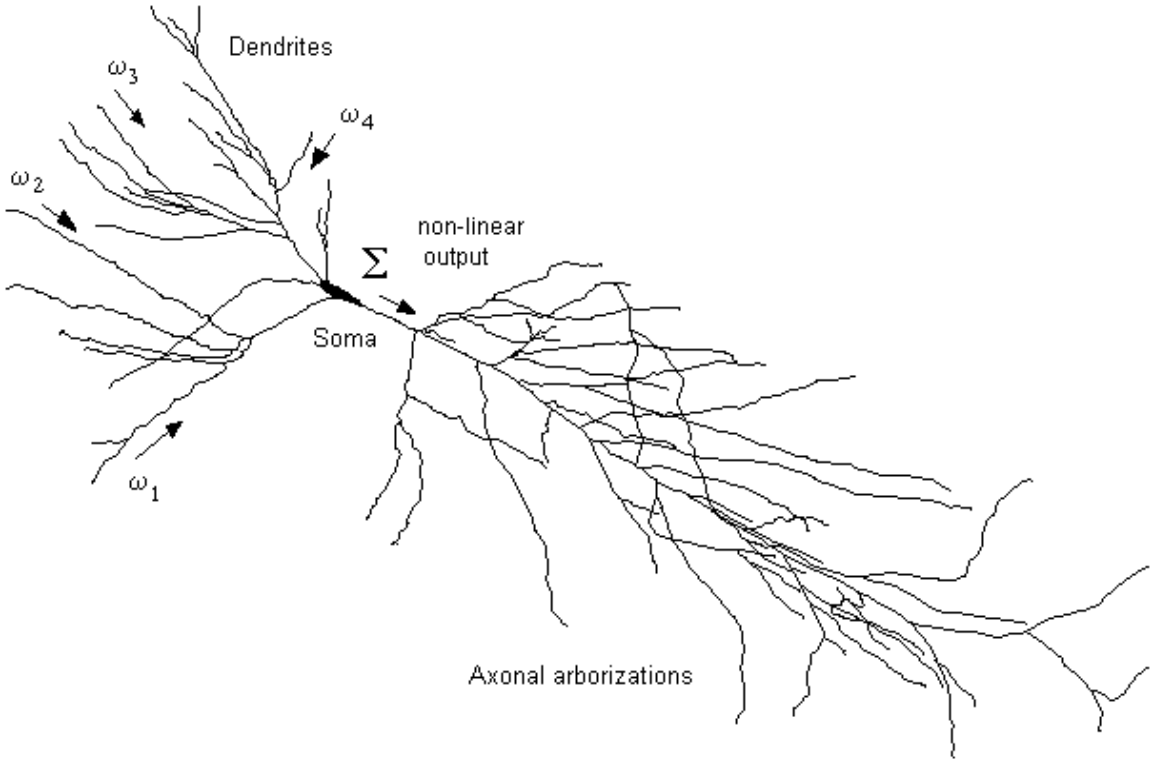

FIG 14 Standard model of informational processing. Inputs from other neurons are multiplied by the corresponding passive dendritic weights ω1-ω4, summed (Σ) and then passed through nonlinearity.

2.5 Axons

When the voltage change in the axonal hillock reaches a threshold potential of -55mV, action potential is triggered. The membrane becomes depolarized due to gate opening of voltage sensitive Na^+ channels, which allow Na^+ to rush into cell. This is an all-or-none event – it ineluctably happens once threshold is reached. When the inside of membrane is depolarized to +40mV, Na^+ gates shut and K^+

gates open. K^+ rushes out trough the open K^+ gates while the Na^+ gates are closed and inactive. The membrane thus becomes repolarized and may even get hyperpolarized. Refractory period occurs while the Na^+ gates of Na^+ channels remain closed: the membrane will not respond again until Na^+ gates become active.

2.5.1 The Hodgkin-Huxley model of axonal firing

The electric current flow across the cell membrane depends on the capacitance of the membrane and the resistance of the ion channels. The total ionic current is represented by the sum of the sodium current, potassium current and a small leakage current. The leakage current represents the collective contribution of ions such as chloride and bicarbonate.

The Hodgkin-Huxley model represents an isopotential membrane patch or a single electrical compartment, i.e., there are no spatial effects on the potential (Hodgkin & Huxley, 1952a; 1952b; 1952c; 1952d; 1952e; 1952f). The units of the model are per membrane unit area, whence it is then straightforward to scale the model to a single compartment of any desired membrane area.

The total membrane current is the sum of the ionic currents and the capacitive current

$$I_m(t) = I_{ionic}(t) + C_M \frac{dV_m(t)}{dt}$$
$$I_{ionic}(t) = I_{Na}(t) + I_K(t) + I_L(t)$$

where I_m is the membrane current density, I_{ionic} are the ionic currents densities, C_M is the membrane capacity per unit area and V_m is the membrane voltage. The two main ionic conductances, sodium and potassium are independent of each other, and a third, leak conductance does not depend on any of the other conductances or the membranal voltage. Thus, the total ionic current is the sum of the separate ionic currents.

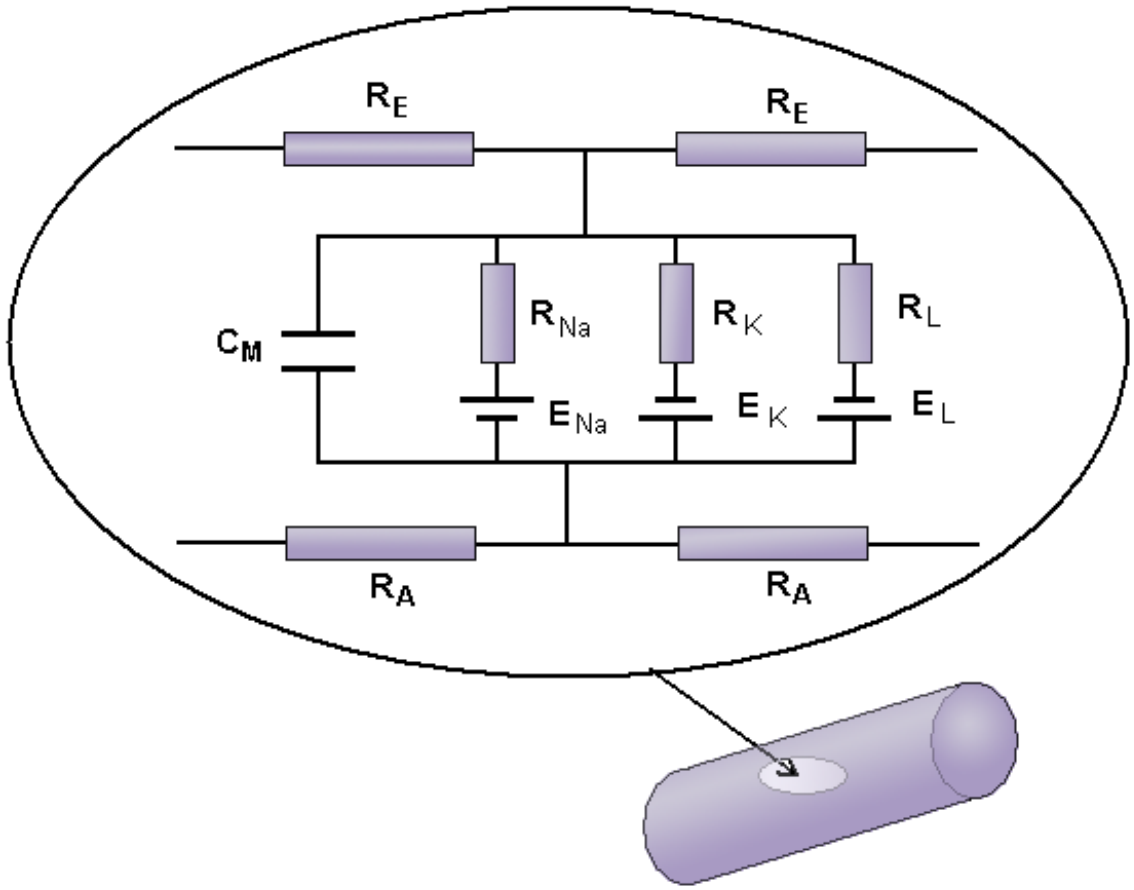

FIG 15 An electrical circuit diagram describing the current flows across the cell membrane that are captured in the Hodgkin-Huxley model. Compare with Fig. 5.

The individual ionic currents are linearly related to the potential according to Ohm's law,

$$I_K(t) = G_K(V,t)\left[V(t) - E_K\right]$$
$$I_{Na}(t) = G_{Na}(V,t)\left[V(t) - E_{Na}\right]$$
$$I_L(t) = G_L(V,t)\left[V(t) - E_L\right]$$

where G_K, G_{Na} and G_L are the potassium, sodium and leak conductances per unit area of the membrane and E_K, E_{Na} and E_L are the corresponding reversal or equilibrium Nernst potentials of each of the ionic species.

The voltage-dependent conductances $G_{Na}(t)$ and $G_K(t)$ are given by

$$G_{Na}(t) = G_{Na}^{\max} f_{Na}(t)$$
$$G_K(t) = G_K^{\max} f_K(t)$$

where $G_{Na}^{\max}$ and $G_{K}^{\max}$ are the peak or maximal sodium and potassium conductances per unit membrane area and $f_{Na}(t)$ and $f_{K}(t)$ are each the corresponding (instantaneous) fraction of the maximal conductance which is actually open (or active). Thus the equation, which describes the membrane potential as a function of all the currents that flow across it, is

$$C_M \frac{dV}{dt} = G_{Na}^{\max} f_{Na}(t)\left[E_{Na} - V(t)\right] + G_{K}^{\max} f_{K}(t)\left[E_{K} - V(t)\right] + \\ + G_{L}^{\max} f_{L}(t)\left[E_{L} - V(t)\right] + I_{injected}(t)$$

The values for some of the parameters are: E_{Na}= +60 mV, $G_{Na}^{\max}$ = 120 mS/cm2, E_K= -93 mV, $G_{K}^{\max}$ = 36 mS/cm2, E_L= -60 mV and $G_{L}^{\max}$ = 0.3 mS/cm2.

The Hodgkin-Huxley model replicates many of the features of spiking of the squid giant axon: the form, duration and amplitude of a single spike (both for the membrane and the propagating spike), its sharp threshold, the conduction velocity of the spike along the axon, the refractory period of the neuron, the impedance changes during the spike, anode-break excitation, accommodation, subthreshold response and oscillations. When simulating the response to sustained stimulus currents, it demonstrates a discontinuous onset of repetitive firing with a high spiking frequency and a limited bandwidth of the firing frequency.

However, careful studies of the model reveal that it does not provide a good description of quite a few electrophysiological properties of the axon (Clay, 1998), in particular the refractory behavior of the preparation in response either to sustained or periodic current pulse stimulation. Also, the model does not account for after potentials and slow changes in the squid giant axon.

Still, the Hodgkin-Huxley model serves as the *golden standard* of neuronal excitability, and with minor changes - as the backbone of most neuronal spiking models. The main reason is that the Hodgkin-Huxley model does capture the essence of spiking through ionic currents (Na^+ and K^+), which enter and leave the cell through voltage dependent channels. Moreover, the model is compact, and approximates well many of the features shared by different types of neurons (shape and duration of spiking, repetitive spiking in response to sustained inputs, refractoriness, etc.) while incorporating biophysical aspects of the neuron. Adding the appropriate currents for other channel types (usually using similar kinetic

schemes) is easily done. Accordingly, and since the model has been studied mathematically in great detail (Jack et al., 1975), it is the common choice of conductance based modeling for computational studies and theoretical ones.

2.5.2 Passive axonal properties

In this section we will pay attention once more on the fact that in every neuronal electric process both active and passive events are involved. The passive spread of the electric currents and electric field happens very fast. These processes can be well described if we take the membrane resistance and capacitance as constant in time. In contrast, the active processes rely on changes in membrane conductivity via gating of ion channels sensitive to voltage.

The action potential generated at the axonal hillock propagates down the axon because of the opening of voltage gated sodium channels. Because the soma and nearby dendrites lack proper distribution of voltage gated ion channels, the action potential does not propagate actively in retrograde direction – or if it does, as we have seen in the previous section when discussing active dendritic properties, it is rare event so that the antidromic (retrograde) propagation of the action potential helps in establishing long-term potentiation (LTP) in dendrites. The passive spread of electric field, however, cannot be prevented. Its depth of penetration depends on the space constant λ, which increases with the increase of the membrane resistance. Conversely, if the membrane resistance is low, ionic leakage through the membrane occurs and the voltage drops faster because λ decreases; at this point one should remember that the space constant λ has the meaning of the distance at which the applied voltage drops e = 2.72 times. On the next picture it is presented a stretch-receptive neuron from crayfish, with dendrites terminating on a muscle fiber. Both dendritic EPSP and IPSP spread are depicted, as well as the retrograde passive spread of the action potential.

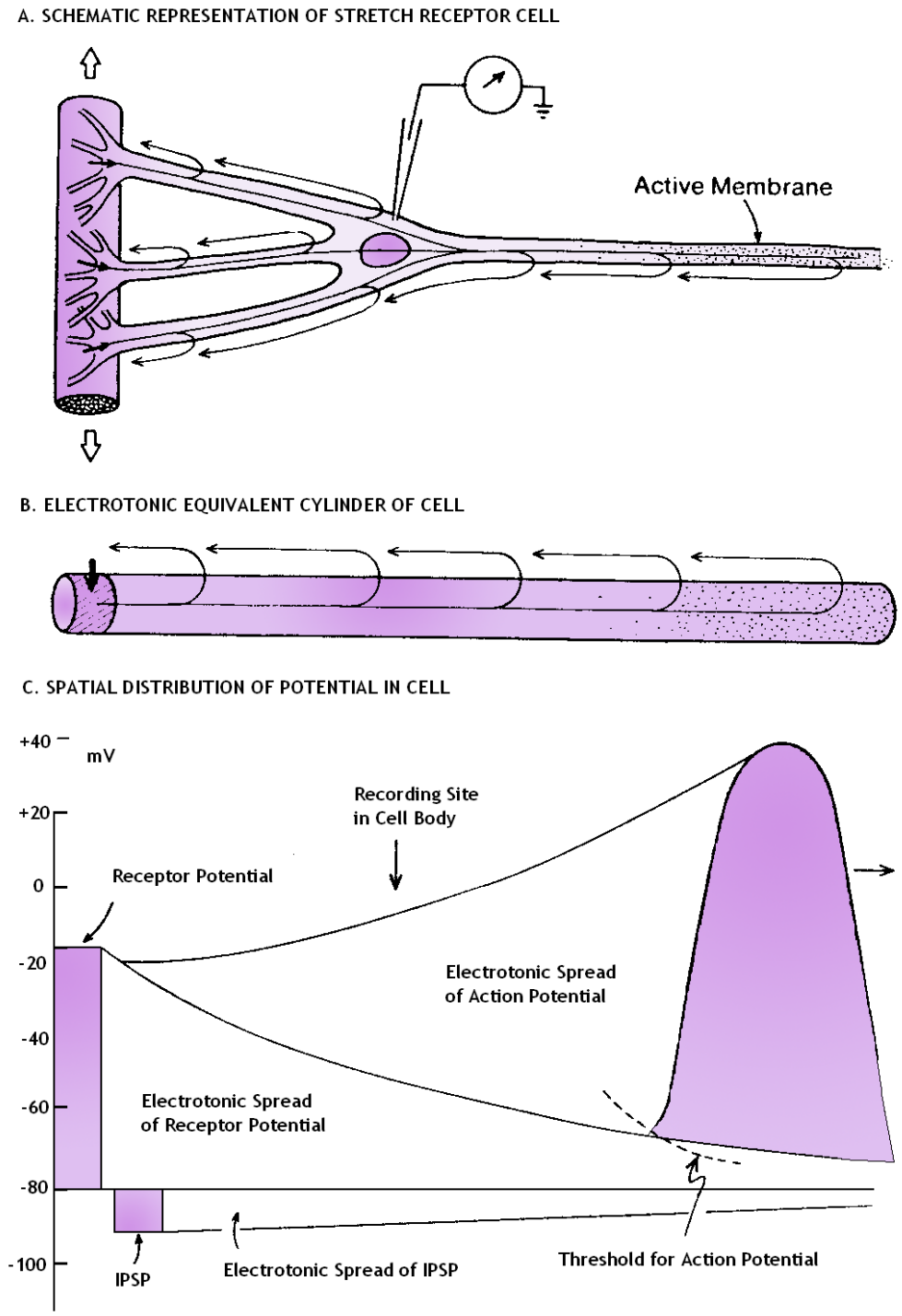

FIG 16 Stretch receptor neuron of the crayfish. The receptive neuron has several large dendritic trunks, which enter the muscle and terminate in fine branches. When stretch is applied to the muscle, a depolarization is set up in the dendritic branches, graded with the amount of stretch.

2.5.3 Electric intensity in the axonal cytoplasm

It would be naïve to expect extreme electric field intensities in the axon compared to the field intensity in dendrites. This is because the *space constant* λ in axons is 1-2 orders of magnitude larger than the dendritic space constant and λ is inversely linked to the electric field strength $\vec{E} = -\nabla V$. The electric field intensity could be approximated by using the cable equation after assessing the space constant λ for the axonal projection – that increases with the diameter of the neuronal projection:

$$\lambda = \sqrt{\frac{dR_M}{4R_A}} = \sqrt{\frac{2.5\times10^{-5} m \times 10\Omega.m^2}{4\times 0.62\Omega.m}} \approx 10mm$$

The applied voltage during action potential is about 120 mV (assuming that a resting membrane of -70 mV is depolarized till the potential reaches +50 mV), so the electric field intensity $\vec{E}$ is about 12 V/m.

2.5.4 Magnetic flux density in axonal cytoplasm

The vector of the magnetic induction $\vec{B}$ will form closed loops around the axis of the neuronal projection. Their direction is defined by the right-handed screw rule (i.e. counterclockwise if the axial current flows toward your face). In axons the magnetic field is stronger than the magnetic field in dendrites because of the greater ion currents flowing inside the axoplasm. The nerve action potential has the form of a moving *solitary wave*, with *peak currents* range from 5 to 10 μA (Katz, B., 1966). Axons range in diameter from less than 1 μm to 25 μm in humans, but reach gigantic size in squid with d = 1mm. Calculations of the magnetic flux density in the largest human axons that have the greatest electric currents give us:

$$\oint_{\Gamma} B \cdot dl = \mu_0 i$$

$$B = \mu_{eff}\mu_0 \frac{i}{\pi d} = \frac{10\times 4\times 10^{-7} H.m^{-1} \times 10^{-6} A}{2.5\times 10^{-5} m} = 1.6\times 10^{-7} T$$

Although this result is 3 orders of magnitude greater than the experimentally measured magnetic field in frog sciatic nerve using SQUID magnetometer (Wikswo et al., 1980) it remains too weak - only $^{1}/_{300}$ of the Earth's magnetic field. The experimentally measured value for the magnetic field $\vec{B}$ of the frog

sciatic nerve using SQUID magnetometer was 1.2×10^{-10} T with a signal-to-noise ratio 40 to 1 (Wikswo et al., 1980). The assessed value for magnetic field strength at the frog nerve surface (where it has peak magnitude) using the Ampere's law was 1.2×10^{-10} T because of large frog sciatic the nerve diameter (d = 0.6mm).

2.6 Electric fields in membranes

The *longitudinal electric intensity* $\vec{E}_L$ and the magnetic flux density in membranes are expected to be the same as the calculated values for the cytoplasm i.e. $\vec{E}_L = 10\ \mathrm{V/m}$ and $\vec{B} = 10^{-7}\ T$. We have seen, however, that the relevant stimulus for the voltage gated ion channels is the *transmembrane voltage* V_m. While its absolute values reach V = 90 mV the intensity of the *transversal electric field* $\vec{E}_T$ is tremendous because of the narrowness of the plasma membrane, which is about 10 nanometers thick. Simple calculations yield

$$\vec{E}_T = -\nabla V = \frac{V}{h} = \frac{9\times10^{-2} V}{10^{-8} m} = 9\times10^{6}\ V/m\ ,$$

where h is the membrane thickness and V is the transmembrane voltage.

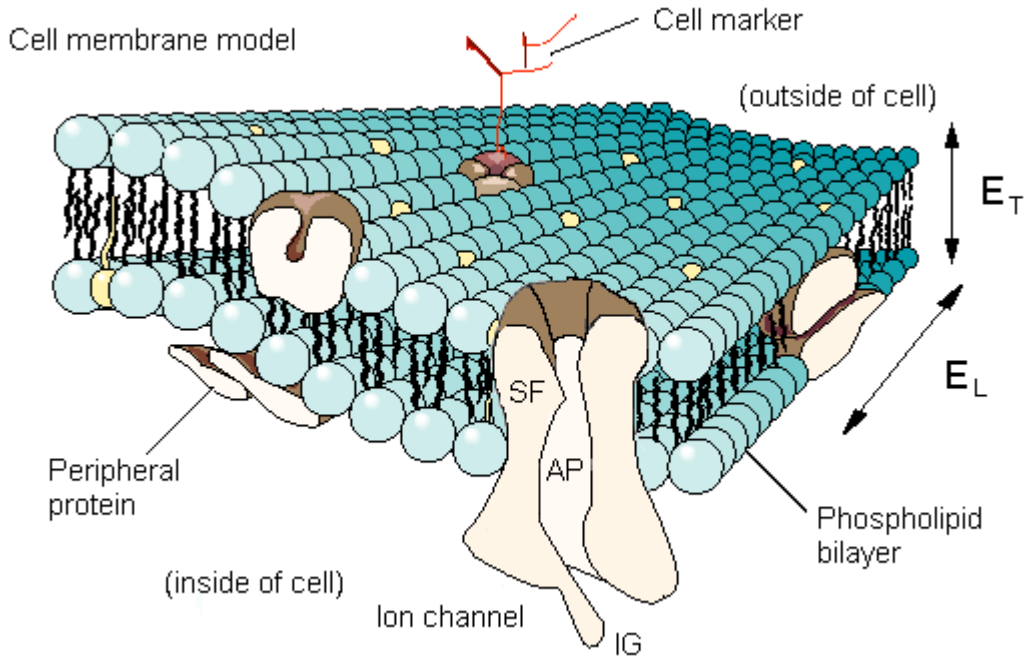

FIG 17 Transversal and longitudinal intensity of the electric field in membranes.

References

Akaike, N. & Moorhouse, A.J. (2003). Techniques: Applications of the nerve-bouton preparation in neuropharmacology. Trends in Pharmacological Sciences 24: 44-47.

Akaike, N. et al. (2002). Focal stimulation of single GABAergic presynaptic boutons on the rat hippocampal neuron. Neurosci. Res. 42: 187-195.

Alberti, A. (1884). Contribución al estudio de las Localizaciones Cerebrales y a la Patogénesis de la Epilepsia. 31 July 1884 Public Concourse, Círculo Médico Argentino, Buenos Aires, Ms.

Alberti, A. (1886). Contribución al estudio de las Localizaciones Cerebrales y a la Patogénesis de la Epilepsia. Buenos Aires, Biedma.

Arfken, G. (1985). "Gradient, ∇" and "Successive Applications of ∇." §1.6 and 1.9 in Mathematical Methods for Physicists, 3rd ed. Orlando, FL: Academic Press, pp. 33-37 and 47-51.

Ávila, A. & Funes, J. (1980), Engramación por islotes de electreto: estudio experimental de su posibilidad como mecanismo neural. Investigación # 6776, Facultad de Medicina de la Universidad de Buenos Aires; progress report in "Guía de Invest. en curso en la Universidad de Buenos Aires vol. II", 1984 : Instituto Bibliotecológico de la Universidad de B. Aires.

Baker, P.F., Hodgkin, A.L., Shaw, T.I. (1961). Replacement of the protoplasm of a giant nerve fibre with artificial solutions. Nature 190: 885-887.

Baker, P.F., Hodgkin, A.L. & Shaw, T.I. (1962a). Replacement of the axoplasm of giant nerve fibres with artificial solutions. J Physiol. 164: 330-354.

Baker, P.F., Hodgkin, A.L. & Shaw, T.I. (1962b). The effects of changes in internal ionic concentrations on the electrical properties of perfused giant axons. J Physiol. 164: 355-374.

Baker, P.F., Hodgkin, A.L. & Meves, H. (1964). The effect of diluting the internal solution on the electrical properties of a perfused giant axon. J Physiol. 170: 541-560.

Barlaro, P. M. (lessons' transcriber) (1909). Curso sobre enfermedades del Sistema Nervioso en relación con su Anatomía Patológica, dictado por el Dr. Chr. Jakob en la Clínica del Dr. Ramos Mejía y recogidas por el Dr. Pablo M. Barlaro, ayudante de Patología Interna. Buenos Aires, La Ciencia Médica.

Beer, B. (1902). Über das Auftrafen einer objective Lichtempfindung in magnetischen Felde. Klin. Wochenschr. 15:108-109.

Bekkers, J.M. (2000). Distribution of slow AHP channels on hippocampal CA1 pyramidal neurons. J. Neurophysiol. 83: 1756-1759.

Caldwell, J.H., Schaller, K.L., Lasher, R.S., Peles, E. & Levinson, S.R. (2000). Sodium channel Nav1.6 is localized at nodes of Ranvier, dendrites, and synapses. PNAS 97(10): 5616–5620

Cauller, L. (2003). Course in Neurophysiology.
Web source: http://www.utdallas.edu/~lcauller/

Chang, H.T. (1952). Cortical neurons with particular reference to the apical dendrites. Cold Spring Harbor Syrnp. Quant. Biol. 17: 189-202.

Christie, B.R. (1995). Different Ca^{2+} channels in soma and dendrites of hippocampal pyramidal neurons mediate spike-induced Ca^{2+} influx. J Neurophysiol. 73(6): 2553-2557.

Clay, J.R. (1998). Excitability of the squid giant axon revisited. J.Neurophysiol., 80:903-913.

Cole, K.S. & Curtis, H.J. (1939). Electric impedance of the squid giant axon during activity. Journal of General Physiology 22: 649-670.

Coss, R.G. & Globus, A. (1978). Spine stems on tectal interneurons in jewel fish are shortened by social stimulation. Science 200: 787- 790.

Crocco, M. F. (1994). Alberto Alberti y el primer mapeo con electricidad ¡durante ocho meses! de un cerebro humano consciente: hazaña científica silenciada durante un siglo. Electroneurobiología 1 (3), 73-82 (September).
Web source: http://electroneubio.secyt.gov.ar/general.htm

Crocco, M. & Contreras, N. (1986a). Oscuridades, enigmas, y el aporte fundamental de Ricardo Sudnik (1880/4) en el origen de la neurobiología argentina. La Semana Médica 168 # 5376 (12 March 1986).

Crocco, M. & Contreras, N. (1986b). El contexto histórico y los descubrimientos de Alberto Alberti en las localizaciones cerebrales. La Semana Médica 168, # 5378 (5 April 1986), 217-230.

Curtis, H.J. & Cole, K.S. (1940). Membrane action potentials from the squid giant axon. J. Cell. Comp. Physiol. 15: 147-157

Curtis, H.J. & Cole, K.S. (1942). Membrane resting and action potentials from the squid giant axon. J. Cell. Comp. Physiol. 19: 135-144.

d'Arsonval, A. (1896) Dispositifs pour la mesure des courants alternatifs de toutes fréquences. C. R. Soc. de Biologie (Paris) 3:450-457.

Diamond, J., Gray, E.G. & Yasargil, G.M. (1970). The function of the dendritic spines: a hypothesis. In P. Anderson and J.K.S. Jansen (Eds.), Excitatory Synaptic Mechanisms, Universitetsforlaget, Oslo, pp. 213-222.

Du Bois-Reymond, E. (1848). Untersuchungen über thierische Elektricität, Erster Band. Berlin: Georg Reimer. The book can be downloaded from Max Planck Institute for the History of Science (806 pages, high resolution, ~180.24 MB).
Web source: http://vlp.mpiwg-berlin.mpg.de/library/pdf/lit92__Hi.pdf

Fleshman, J.W., Segev, I. & Burke, R.B. (1988). Electrotonic architecture of type-identified α-motoneurons in the cat spinal cord. Journal of Neurophysiology 60: 60-85.

Frick, P., Khripchenko, S., Denisov, S., Sokoloff, D. & Pinton, J.F. (2003). Effective magnetic permeability of a turbulent fluid with macroferroparticles. EPJ manuscript.
Web source: http://www.ens-lyon.fr/~pinton/ARTICLES/mhd_SB_EPJB.pdf

Galvani, L. (1791). De viribus electricitatis in motu musculari, Bologna. (Translated in english: Galvani, Luigi. Commentary on the Effects of Electricity on Muscular Motion. Norwalk, CT, 1953. 176 pp., 4 folding plates, illus. Includes facsimile and translation of Galvani's De viribus electricitatis in motu musculari, Bologna, 1791, plus a bibliographical study by John F. Fulton and Madeline E. Stanton.)

Georgiev, D. (2003). Electric and magnetic fields inside neurons and their impact upon the cytoskeletal microtubules.
Web source: http://cogprints.ecs.soton.ac.uk/archive/00003190/

Golding, N.L. & Spruston, N. (1998). Dendritic sodium spikes are variable triggers of axonal action potentials in hippocampal CA1 pyramidal neurons. Neuron. 21: 1189-1200.

Golding, N.L., Jung, H.Y., Mickus, T. & Spruston N. (1999). Dendritic calcium spike initiation and repolarization are controlled by distinct potassium channel subtypes in CA1 pyramidal neurons. J Neurosci. 19: 8789-8798.

Golding, N.L., Kath, W.L. & Spruston N. (2001). Dichotomy of action-potential backpropagation in CA1 pyramidal neuron dendrites. J Neurophysiol. 86: 2998-3010.

Hodgkin, A.L. & Huxley, A.F. (1952a). Currents carried by the sodium and potassium ion through the membrane of the giant axon of Loligo. J. Physiol. 116(4): 449-472.

Hodgkin, A.L. & Huxley, A.F. (1952b). The components of the membrane conductance in the giant axon of the Loligo. J. Physiol. 116(4): 473-496.

Hodgkin, A.L. & Huxley, A.F. (1952c). The dual effect of membrane potential on sodium conductance in the giant axon of Loligo. J. Physiol. 116(4): 497-506.

Hodgkin, A.L. & Huxley, A.F. (1952d). A quantitative description of membrane current and its application to conduction and excitation in nerve. J Physiol. 117(4): 500-544.

Hodgkin, A.L. & Huxley, A.F. (1952e). Propagation of electrical signals along giant nerve fibers. Proc R Soc Lond B Biol Sci. 140(899): 177-183.

Hodgkin, A.L. & Huxley, A.F. (1952f). Movement of sodium and potassium ions during nervous activity. Cold Spring Harb Symp Quant Biol. 17: 43-52.

Hoffman, D.A., Magee, J.C., Colbert, C.M. & Johnston, D. (1997). K^+ channel regulation of signal propagation in dendrites of hippocampal pyramidal neurons. Nature. 387: 869-875.

The IUPHAR Compendium of Voltage-gated Ion Channels, 2002.
Web source: http://www.iuphar-db.org/iuphar-ic/

Jakob, C. (1906, 1907, 1908). "Localización del alma y de la inteligencia", El Libro (Buenos Aires) 1 (1906), 151; and (1907), pp. 281, 433, 553; V. 2 (1908) pp. 3, 171, 293, 537 and 695 (published on nine issues).

Jakob, C. (1911). Vom Tierhirn zum Menschenhirn, I Teil: Tafelwerk nebst Einführung in die Geschichte der Hirnrinde. J. F. Lehmann's Verlag, München.

Jack, J.J.B., Noble, D. & Tsien, R. (1975). Electric current flow in excitable cells. Oxford.

Jaffe, D.B., Johnston, D., Lasser-Ross, N., Lisman, J.E., Miyakawa, H. & Ross, W.N. (1992). The spread of Na+ spikes determines the pattern of dendritic Ca^{2+} entry into hippocampal neurons. Nature. 357: 244-246.

Jaffe, L.F. & Nuccitelli, R. (1977). Electrical controls of development. Annual Review of Biophysics and Bioengineering 6: 445-476.

Jung, H.Y., Mickus, T. & Spruston, N. (1997). Prolonged sodium channel inactivation contributes to dendritic action potential attenuation in hippocampal pyramidal neurons. J Neurosci. 17: 6639-6646.

Kaplan, W. (1991). "The Gradient Field". §3.3 in Advanced Calculus, 4th ed. Reading, MA: Addison-Wesley, pp. 183-185.

Katz, B. (1966). Nerve, Muscle and Synapse. McGraw-Hilt, New York.

Kirischuk, S. et al. (1999). Relationship between presynaptic calcium transients and postsynaptic currents at single GABAergic boutons. PNAS 96: 7520-7525.

Lamacq, L. (1897). Les centres moteurs corticaux du cerveau humain déterminés d'aprés les effets de l'excitation faradique des hémisphères cérébraux de l'homme. Arch. Clin. Bordeaux 6, 11-13 (novembre).

Lancaster, B. & Adams, P.R. (1986). Calcium-dependent current generating the afterhyperpolarization of hippocampal neurons. J. Neurophysiol. 55: 1268-1282.

Lipowsky, R., Gillessen, T. & Alzheimer, C. (1996). Dendritic Na+ channels amplify EPSPs in hippocampal CA1 pyramidal cells. J Neurophysiol. 76: 2181-2191.

Llinas, R. & Hess, R. (1976). Tetrodotoxin-resistant dendritic spikes in avian Purkinje cells. Proc. Natl. Acad. Sci. USA 73: 2520-2523.

Llinas, R. & Nicholson, C. (1971). Electroresponsive properties of dendrites and somata in alligator Purkinje cells. J. Neurophysiol. 34: 532-551.

Llinas, R. & Sugimori, M. (1980). Electrophysiological properties of in vitro Purkinje cell dendrites in mammalian cerebellar slices. J. Physiol. 305: 197-213.

London, M. & Segev, I. (2001). Synaptic scaling in vitro and in vivo. Nature Neuroscience 4(9): 853-854.
Web source: http://lobster.ls.huji.ac.il/idan/files/London_Segev_NN2001.pdf

Magee, J.C. (1999). Dendritic Ih normalizes temporal summation in hippocampal CA1 neurons. Nat. Neurosci. 2(9): 848.

Magee, J.C. & Cook, E.P. (2000). Somatic EPSP amplitude is independent of synapse location in hippocampal pyramidal neurons. Nat Neurosci. 3(9): 895-903. Web source:
http://www.medicine.mcgill.ca/physio/pdf_files/Cook/mageeCook_895_200.pdf

Magee, J.C. & Johnston, D. (1995). Characterization of single voltage-gated Na^+ and Ca^{2+} channels in apical dendrites of rat CA1 pyramidal neurons. J Physiol (Lond). 487: 67-90.

Matteucci, C. (1838). Sur le courant electrique ou propre de la grenouille; second mémoire sur l'electricité animale, faisant suite à celui sur la torpille. Paris.

Matteucci, C. (1840). Essai sur les phénomènes électriques des animaux. Paris.

Matteucci, C. (1844). Traité des phénomènes électro-physiologiques des animaux. Paris.

Mayer, M.L. & Vyklicky, L. Jr. (1989). Concanavalin A selectively reduces desensitization of mammalian neuronal quisqualate receptors. PNAS 86: 1411-1415.

Mickus, T., Jung, H. & Spruston, N. (1999). Properties of slow, cumulative sodium channel inactivation in rat hippocampal CA1 pyramidal neurons. Biophys J. 76: 846-860.

Miller, J.P. (1980). Cytoplasmic resistivity of neurons in the lobster stomatogastric ganglion.
Web source: http://cns.montana.edu/~zane/Cytoplasmic.htm

Miller, J.P., Rall, W., & Rinzel, J. (1985). Synaptic amplification by active membrane in dendritic spines. Brain Res.325: 325-330.
Web source: http://cns.montana.edu/research/pub/synamp85/

Mills, L.R., Niesen, C.E., So, A.P., Carlen, P.L., Spigelman, I. & Jones, O.T. (1994). N-type Ca2+ channels are located on somata, dendrites, and a subpopulation of dendritic spines on live hippocampal pyramidal neurons. J Neurosci. 14: 6815-6824.

Morse, P.M. & Feshbach, H. (1953). "The Gradient." In Methods of Theoretical Physics, Part I. New York: McGraw-Hill, pp. 31-32.

Nave, C.R. (2003). HyperPhysics.
Web source: http://hyperphysics.phy-astr.gsu.edu/hbase/hph.html

Nernst, W.H. (1888). Zur Kinetik der Lösung befindlichen Körper: Theorie der Diffusion. Z. Phys. Chem. 3: 613-37.

Nernst, W.H. (1889). Die elektromotorische Wirksamkeit der Ionen. Z. Phys. Chem. 4: 129-81.

Neuron DB database is being developed by Luis N. Marenco[1], Buqing Mao[1], Chiquito Crasto[1], Prakash M. Nadkarni[1], Perry L. Miller[1] and Gordon M. Shepherd[2]; [1]Center for Medical Informatics; [2]Section of Neurobiology; Yale University School of Medicine, New Haven, CT 06510. Supported by NIDCD, NASA, & NIMH (Human Brain Project) and the National Library of Medicine's IAIMS Program.
Web source: http://senselab.med.yale.edu/senselab/NeuronDB/

Olhoeft, G.R. (2003). Electromagnetic Wave Propagation Velocity.
Web source: http://www.g-p-r.com/velocity.htm

Petrolli, G. (2001). Alberto Alberti, neurochirurgo ítalo-argentino. Edizioni Stella, Nicolodi Editore, Roveretto, Italia.

Pike, L.J. (2003). Lipid rafts: bringing order to chaos. J. Lipid Res. 44: 655-667.

Sajda, P. (2002). Computational Neural Modeling and Neuroengineering. BMEN E6480. Lecture 2: Cable Theory and Dendritic Trees.
Web source: http://www.bme.columbia.edu/~sajda/bme6480/

Sayer, R.J., Friedlander, M.J. & Redman, S.J. (1990). The time course and amplitude of EPSPs evoked at synapses between pairs of CA3/CA1 neurons in the hippocampal slice. J. Neurosci. 10: 826-836.
Web source: http://www.jneurosci.org/cgi/content/abstract/10/3/826

Schey, H.M. (1997). Div, Grad, Curl, and All That: An Informal Text on Vector Calculus, 3rd ed. New York: W. W. Norton.

Shao, L.R., Halvorsrud, R., Borg-Graham, L. & Storm, J.F. (1999). The role of BK-type Ca^{2+}-dependent K^+ channels in spike broadening during repetitive firing in rat hippocampal pyramidal cells. J. Physiol. 521: 135-146.

Shepherd, G.M. (1994). Neurobiology, Third Edition. Oxford U. Press, New York.

Shepherd, G.M. & Brayton, R.K. (1987). Logic operations are properties of computer-simulated interactions between excitable dendritic spines. Neuroscience 21(1): 151-165.

Spencer, W.A. & Kandel, E.R. (1961). Electrophysiology of the hippocampal neurons. IV. Fast prepotentials. J Neurophysiol. 24: 272-285.

Spruston, N. (2000). Distant synapses raise their voices. Nature Neuroscience 3: 849-851.

Spruston, N. & Johnston, D. (1992). Perforated patch-clamp analysis of the passive membrane properties of three classes of hippocampal neurons. J Neurophysiol. 67: 508-529.

Spruston, N., Schiller, Y., Stuart, G. & Sakmann, B. (1995). Activity-dependent action potential invasion and calcium influx into hippocampal CA1 dendrites. Science. 268: 297-300.

Staff, N.P., Jung, H.Y., Thiagarajan, T., Yao, M. & Spruston, N. (2000). Resting and active properties of pyramidal neurons in subiculum and CA1 of rat hippocampus. J Neurophysiol. 84: 2398-2408.

Steinhauser, C., Tennigkeit, M., Matthies, H. & Gundel, J. (1990). Properties of the fast sodium channels in pyramidal neurones isolated from the CA1 and CA3 areas of the hippocampus of postnatal rats. Pflugers Arch. 415: 756-761.

Stocker, M. & Pedarzani, P. (2000). Differential distribution of three Ca^{2+}-activated K^+ channel subunits, SK1, SK2, and SK3, in the adult rat central nervous system. Mol. Cell. Neurosci. 15: 476-493.

Stoilov, S., Rusanov, E., Mitev, D. & Genkov, D. (1985). Biophysics. Publishing house "Medicine & Physical Culture", Sofia.

Tsubokawa, H., Offermanns, S., Simon, M. & Kano, M. (2000). Calcium-dependent persistent facilitation of spike backpropagation in the CA1 pyramidal neurons. J Neurosci. 20: 4878-4884.

von Helmholtz, H. (1850). Über die Fortpflanzungsgeschwindigkeit der Nervenreizung. Arch. Anat. Physiol. Wiss. Med. pp.71-73. This and the two following references are to be soon available on Helmholtz' multivolume *Gesammelte Werke* series being published by Georg Olms Verlag of Hildesheim; web source http://www.olms.de

von Helmholtz, H. (1852). Messungen über Fortpflanzugsgeschwindigkeit der Reizung iun Nerven. Arch. Anat. Physiol. Wiss. Medizin. pp.199-216

von Helmholtz, H. (1854). Uber die geschwindigkeit einiger vorgange in muskeln und nerve. Bericht über die zur bekanntmachung geeigneten verhandlungen der koniglichen. Preuss Akad Wiss., Berlin. pp. 328-332

Waldrop, B. & Glantz, R.M. (1985). Synaptic mechanisms of a tonic EPSP in crustacean visual interneurons: analysis and simulation. Journal of Neurophysiology 54: 636-650.

Weisstein, E.W. (2003). Gradient. Wolfram Research, Inc.
Web source: http://mathworld.wolfram.com/Gradient.html

Westenbroek, R.E., Ahlijanian, M.K. & Catterall, W.A. (1990). Clustering of L-type Ca^{2+} channels at the base of major dendrites in hippocampal pyramidal neurons. Nature. 347: 281-284.

Wikswo, J.P., Barach, J.P. & Freeman, J.A. (1980). Magnetic Field of a Nerve Impulse: First Measurements. Science 208: 53-55.
Web source: http://www.vanderbilt.edu/lsp/abstracts/wikswo-s-1980.htm

Yuste, R. & Tank, D.W. (1996). Dendritic Integration in Mammalian Neurons, a Century after Cajal. Neuron 16: 701-716.

Zlatev, M.P. (1972). Theoretical Electrotechnics. Volume I. Publishing house "Technics", Sofia.

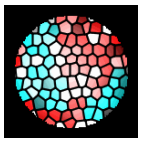

revista
Electroneurobiología
ISSN: 0328-0446